1 OF 1

AD
A069433

HYDROTHERMAL MODELLING OF BROWNS FERRY
NUCLEAR PLANT COOLING TOWERS

by

Subhash C. Jain and John F. Kennedy

LEVEL II

D D C

JUN 6 1979

A

79 05 31 026

HYDROTHERMAL MODELLING OF BROWNS FERRY NUCLEAR PLANT COOLING TOWERS

by

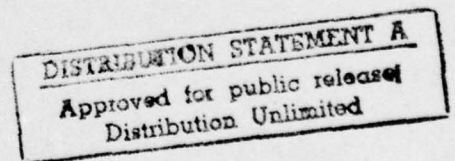Subhash C. Jain and John F. Kennedy

188 300

LB

Acknowledgements

i

ABSTRACT

A laboratory model study of the mechanical draft cooling towers of Browns Ferry Nuclear Plant was conducted to determine plume recirculation and cooling-tower interference quantitatively, and to evaluate the effectiveness of various modifications, including removal of a nearby spoil hillock, rearrangement of the tower cells, and increase of stack height, on the cooling-tower performance. Two sectional models with a scale of 1:150, each consisting of two towers, were tested. The dynamic scaling was based on equality of the densimetric Froude number, F_D, ($F_D = V_j / \sqrt{(\Delta\rho_o/\rho_a)gD}$, where V_j is the stack exit velocity, D is the stack diameter, g is the gravitational constant, ρ_a is the ambient fluid density and $\Delta\rho_o$ is the density difference between the ambient and jet effluent) and the velocity ratio K ($K = V_j/V_a$, where V_a is the cross-flow velocity at the stack height). It was found that the effect of the spoil hill and of the relocation of two cells per tower on the overall recirculation ratio of the towers is not significant. An increase in stack height from 14 ft to 42 ft significantly reduced tower recirculation.

$F(D), (F(D) = V(J) / sq. root of delta(Rho sub o) g D$

rho sub a

delta (Rho sub o)

Table of Contents

List of Tables

List of Figures

HYDROTHERMAL MODELLING OF BROWNS FERRY
NUCLEAR PLANT COOLING TOWERS

I. INTRODUCTION

TVA's Browns Ferry Nuclear Plant is fitted with six 16-cell, rectlinear, mechanical-draft cooling towers (figure 1) which are operated in the closed-cycle and helper modes of the condenser cooling system of this 3,456 MW generating station which is located along the right shore of Wheeler Reservoir near Decatur, Alabama. The cooling towers have failed to meet the design requirements (Waldrop et al. 1977), with the result that during some summer months it is necessary to derate the plant or to be at variance with the numerical thermal criteria adopted for Wheeler Reservoir. For this reason, TVA initiated an investigation to determine modifications which would improve the performance of the cooling towers.

The laboratory model study reported herein was undertaken to determine the extent to which plume recirculation and cooling-tower interference (Chen et al. 1974) were contributing to the performance short-fall of the towers, and to evaluate the effectiveness of the following measures in improving cooling-tower performance.

1. Removal of the spoil hillock (formed by dumping of material excavated during construction of the towers and the canals) on the east side of the towers (see figure 1).

2. Rearrangement of the tower cells to form more, shorter towers, and thereby improve the air flow to the downwind sides of the towers.

3. Increase of stack height, to reduce recirculation.
The effects of the modifications on the cooling performance of the tower were evaluated by measuring the amount of stack effluent ingested by the towers, as explained in the following section. The potential for downwind fogging was evaluated for some conditions by measuring the downwind distribution of stack-effluent concentration.

1" = 600'

0 300 600
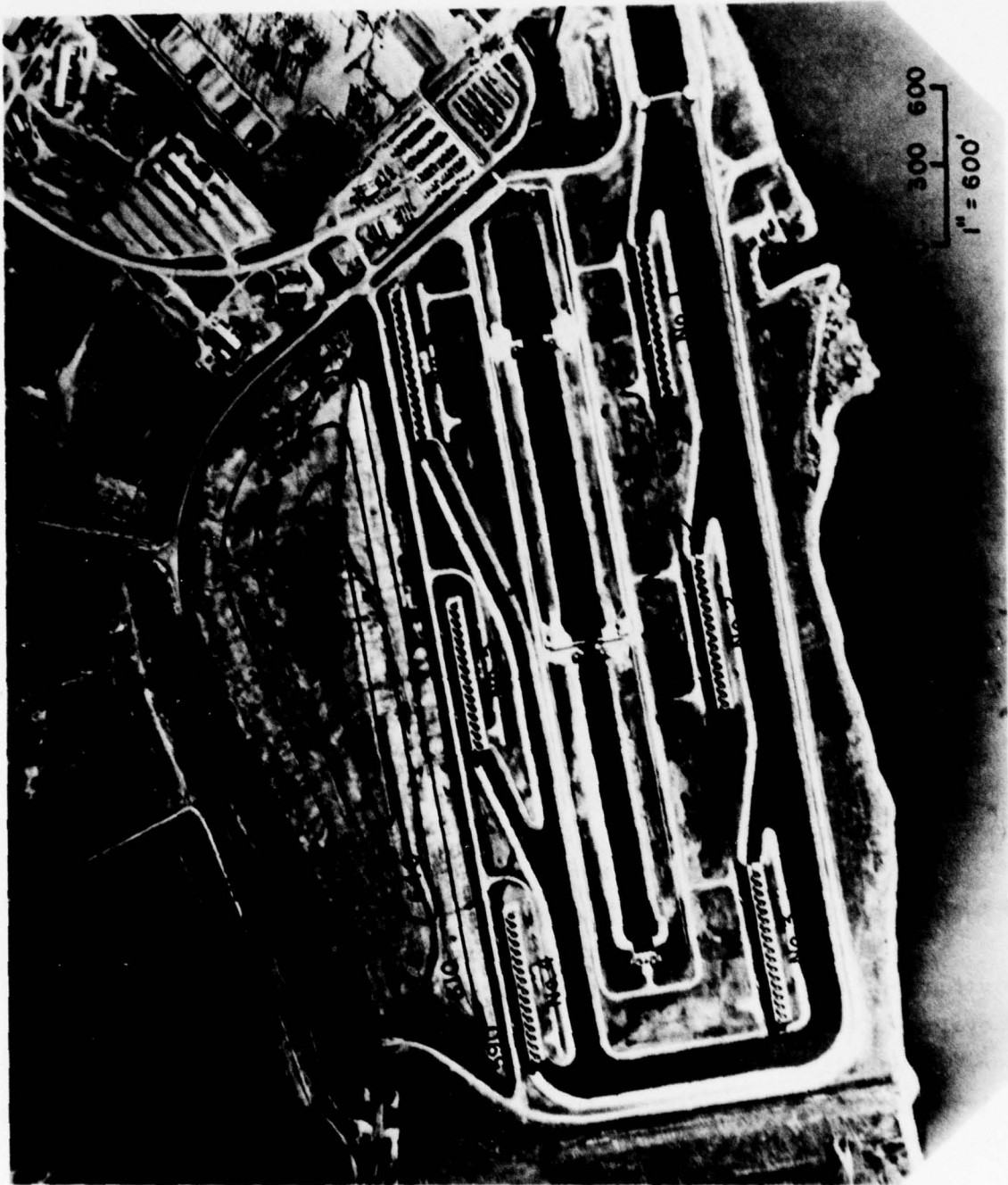
Figure 1. Layout plan of cooling towers and the spoil hill

II.   RECIRCULATION AND INTERFERENCE

Figure 2 depicts schematically a cross-section through a rectilinear cooling tower in a cross-wind. The forced plumes leave the stacks with moderately high velocity (35 ft/sec for the Browns Ferry towers), and entrain and become diluted by surrounding air. Here it should be noted that the cross-wind markedly increases the rate of entrainment of ambient air by the plume. The cross-flow has two other significant effects. First, it deflects the trajectory of the plume; and second it produces a wake with large captive eddies on the lee side of the tower. The wake eddies entrain stack-effluent fluid from the deflected plumes, into the wake region, from where it is withdrawn into the tower as part of the inflow through the lower faces. This ingestion of its own stack effluent by a tower is called recirculation; the recirculation ratio is defined as the fraction of stack effluent in the louver-face inflow. Note that in the absence of a cross-wind, the recirculation ratio is zero unless the plumes have strong negative buoyancy.

Figure 3 depicts the phemonenon of tower interferences,which is the ingestion by a tower of the stack effluent of an upwind tower. The concentration of stack effluent may be particularly high in the captive eddy which forms and persists between closely-spaced towers in the presence of a cross wind. This captive eddy entrains air from the deflected plume of the upwind tower, and leads to ingestion of tower effluent by both the upwind and downwind towers. Accordingly, the recirculation ratio of an upwind tower generally is increased by the presence of the inter-tower wake. Note that the downwind tower generally experiences both interference and recirculation; the combined effect for this tower also is referred to as recirculation.

It is self-evident that recirculation and interference degrade tower performance. The stack-effluent fluid withdrawn into the tower through the louver faces has had its heat-assimilation capacity already utilized by its previous pass through the tower, and therefore can produce no further cooling of the water. Consequently, the temperature of the cold-water leaving the tower is increased, the turbine back-pressure is raised, and turbine efficiency is reduced. As a first, and very rough, approximation, the reduction in cooling capacity can be estimated as equal to the fraction of stack-effluent withdrawn into the tower. That is, a fraction of the cooling-tower capacity
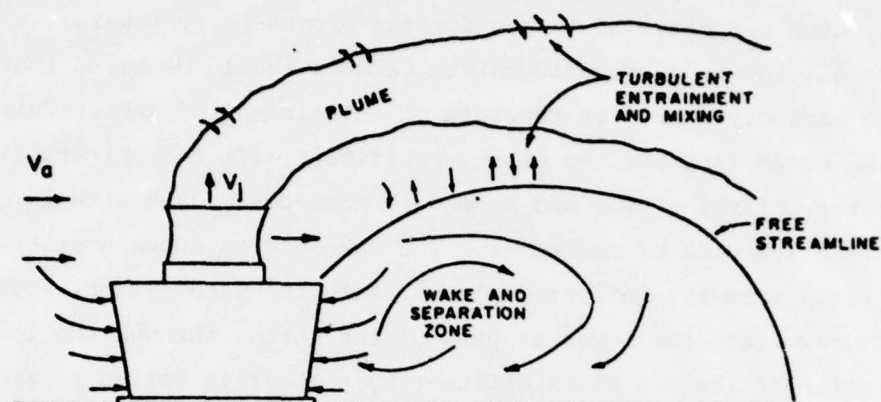
Figure 2.   Schematic depicting recirculation in a
cooling tower
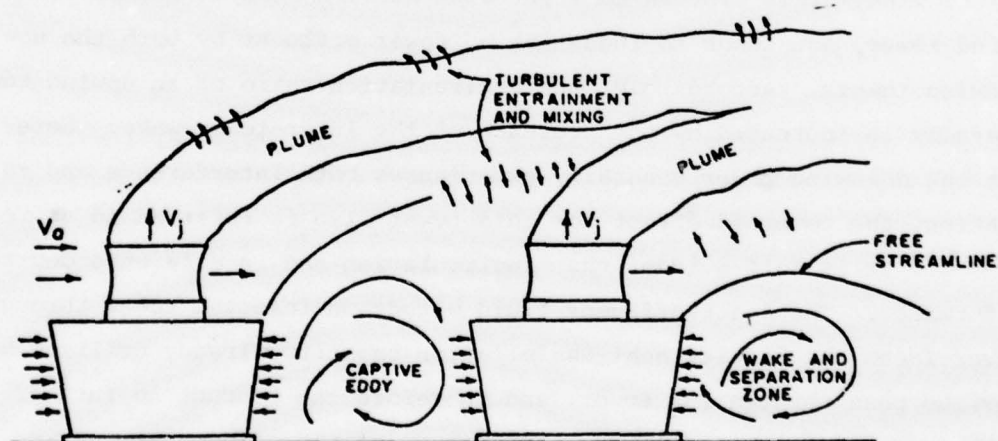
Figure 3.   Schematic illustrating inteference between
cooling towers

roughly equal to the fraction of stack effluent in the ingested air is rendered inactive, and the effective size of the tower is thereby reduced.

III. MODELLING CONSIDERATIONS

Accurate simulation of prototype conditions in a model study requires that certain dimensionless parameters assume equal values in model and prototype. The independent parameters of interest in the study of mechanical draft cooling-tower plume behavior in a neutral (unstratified) atmospheric boundary layer are: H = stack height; D = stack diameter; S = stack spacing; L = length of tower; V_j = stack exit velocity; ρ_j = effluent density; ρ_a = ambient density; V_a = ambient free-stream velocity; θ = wind direction; δ = atmospheric boundary layer thickness; h = typical scale length of the surrounding topographical features; ν_j = kinematic viscosity of the effluent; ν_a = kinematic viscosity of the ambient fluid; and g = gravitational constant. The dependent quantity of primary interest in this investigation is the spatial distribution of the concentration of the stack effluent, or equivalently the relative temperature ratio, $\Delta T/\Delta T_o$, where $\Delta T = T - T_a$; $\Delta T_o = T_j - T_a$; T = temperature at any point in the flow field, T_j = stack exit temperature, and T_a = ambient temperature. Note that $\Delta T/\Delta T_o$ is also the concentration of stack effluent. It can be shown by dimensional analysis

$$\frac{\Delta T}{\Delta T_o} = f(\frac{x}{D}, \frac{y}{D}, \frac{z}{D}, \frac{V_j}{\sqrt{gD}}, \frac{V_j}{V_a}, \frac{V_j D}{\nu_j}, \frac{V_a \delta}{\nu_a}, \frac{\Delta\rho_o}{\rho_a}, \frac{\delta}{D}, \frac{h}{D}, \frac{L}{D}, \frac{H}{D}, \frac{S}{D}, \theta) \quad (1)$$

where x, y, and z are the Cartesian coordinates of any point in the flow field. The neglect of the effect of the density variation in all except the buoyancy term (the Boussinesq approximation) allows $\Delta\rho_o/\rho_a$ to be incorporated into $V_j/\sqrt{gD}$, with the result

$$\frac{\Delta T}{\Delta T_o} = f(\frac{x}{D}, \frac{y}{D}, \frac{z}{D}, F_D, K, \mathbf{R}_j, \mathbf{R}_\delta, \frac{\delta}{D}, \frac{h}{D}, \frac{L}{D}, \frac{H}{D}, \frac{S}{D}, \theta) \quad (2)$$

where

$$F_D = \frac{V_j}{\sqrt{\frac{\Delta\rho_o}{\rho_a} gD}} = \text{jet densimetric Froude number}$$

$$K = \frac{V_j}{V_a} = \text{velocity ratio}$$

$$\mathbb{R}_j = \frac{V_j D}{\nu_j} = \text{jet Reynolds number}$$

$$\mathbb{R}_\delta = \frac{V_a \delta}{\nu_a} = \text{ambient Reynolds number}$$

It is neither necessary nor practical to reproduce the prototype Reynolds numbers exactly in the model, provided that both the ambient and jet flows are fully turbulent. A fully developed turbulent boundary layer with the required thickness and velocity distribution (Counihan 1969) can be produced by installing a suitable boundary-layer fence, vortex generators, and roughness elements suitably arrayed near the upstream end of a flume or wind-tunnel working section. Dynamic similarity is therefore insured when the values of the jet densimetric Froude number F_D, and the velocity ratio, K, are equal in model and prototype, provided $\mathbb{R}_j$ and $\mathbb{R}_\delta$ are above the critical levels and the velocity distribution in the approach flow reproduces the prototype to scale.

Equating the jet densimetric Froude numbers for models and prototype yields

$$V_r = \sqrt{(\left| \Delta \rho_o / \rho_a \right|_r D_r)} \tag{3}$$

where the subscript r denotes the ratio of any two corresponding quantities in model and prototype. Limitations of laboratory facilities generally impose certain restrictions on each of the three ratios appearing in (3). In a laboratory the model could, of course, be studied either in air or water. However, for reasonable values of model scale and density-ratio scale, it turns out that for either air or water the model must be operated at such low velocities that they are difficult to measure in air. On the other hand, the velocities corresponding to practical values of model and density-ratio scales for water are readily measured using miniature propeller meters. Water offers the additional advantage that the required density differences can be produced easily (by heating or cooling), and point concentrations of stack effluent can be measured with temperature sensors.

In an earlier experimental study of recirculation in mechanical draft cooling towers (Chan et al. 1974) it was found that for $K \geq 1$ (which is the range of interest in the present study), recirculation achieves its

higher values for the case in which the cross-wind is either normal to the
tower axes ($\theta = 90°$) or at an angle of 45° to the tower axes ($\theta = 45°$).
Therefore, it was decided to conduct tests only for these two values of θ. It
was also concluded that both the recirculation and interference effects for
these two wind directions could be adequately reproduced using a sectional
model consisting of just two towers. The use of only two towers permitted
a much larger model scale, which also has its advantages. In order to
keep the Reynolds numbers above the critical levels while at the same time
keeping the blockage effects suitably low, a model scale of 1:150 was adopted.
The density-scale ratio was dictated by the available heating capacity and
the experimental facility utilized, and the corresponding velocity scale was
determined from (3). Note that use of the largest available values of the
density-scale ratio not only gives larger model velocities, and thereby
facilitates velocity measurement, but also produces larger point temperature
rises and yields improved accuracy of temperature determination, and therefore
also of the relative temperature ratio (which corresponds to stack-effluent
concentration).

IV. APPARATUS AND PROCEDURE

The experiments were conducted in the Environmental Flow Facility
(EFF) located in the East Annex of the Iowa Institute of Hydraulic Research.
The EFF is a recirculating, free surface flume with a working section 65 ft
(19.81 m) long, 10 ft (3.05 m) wide, and 7.5 ft (2.29 m) deep. Figure 4
shows a schematic diagram of the EFF; it consists of the main pumping system;
the effluent (discharge) supply system; and the intake water withdrawal system.
The ambient flow through the flume is propelled by two 36 in. (91.4 cm)
pumps driven by variable speed motors, and enters the working section of
the flume through a contraction fitted with grids and screens to smooth the
flow. The flume discharge can also be controlled by two valves, one located
above each pump inlet. A maximum discharge of about 42 cfs per pump can be
obtained. The required velocity distribution of the ambient flow (the
atmospheric boundary layer) was produced by means of a boundary layer-fence,
vorticity generators, and surface roughness elements, and was measured with
a miniature propeller meter. A small cooling tower mounted outside the
laboratory building and connected to the flume can be used to control the model
ambient temperature.
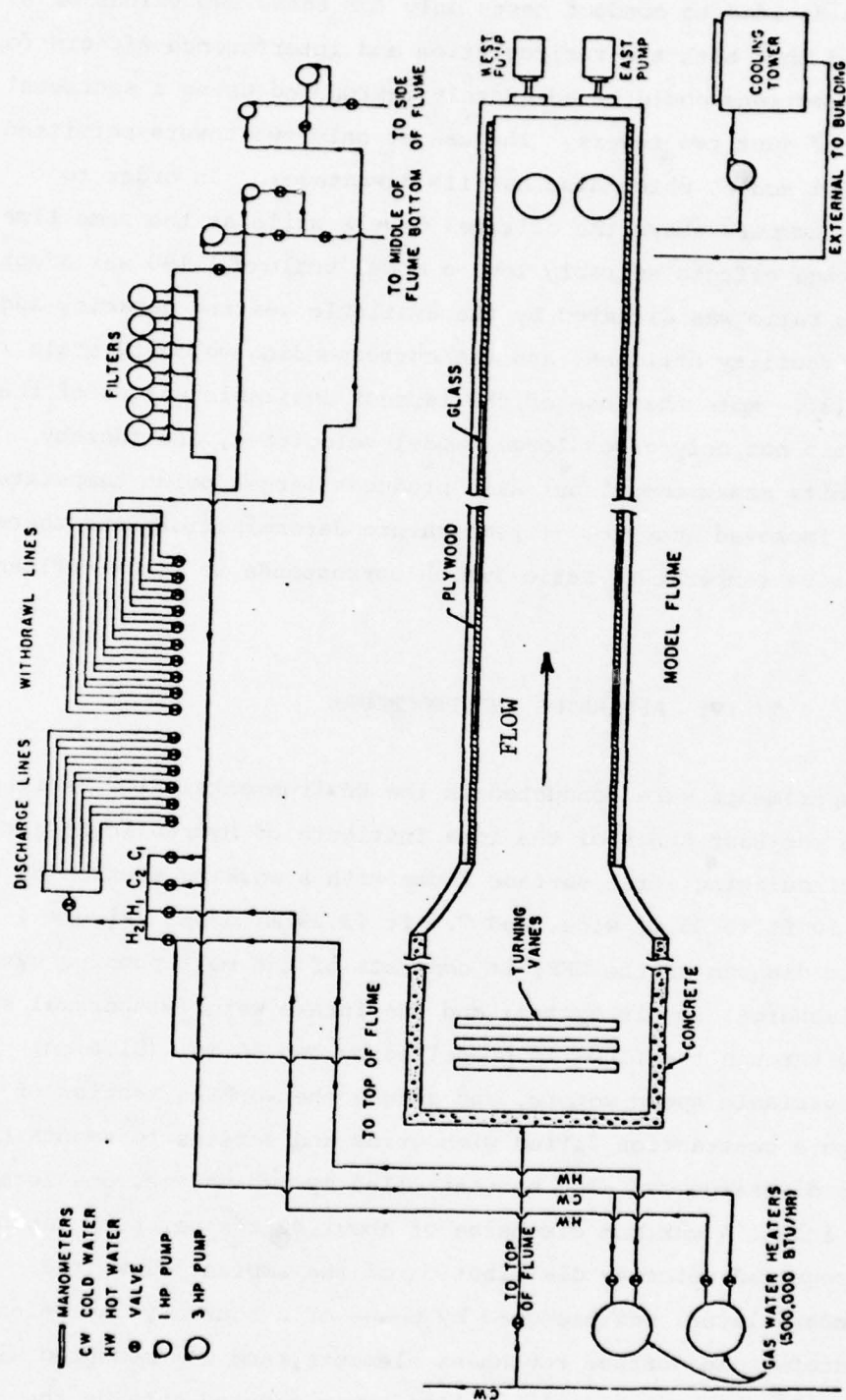
Figure 4. Schematic diagram of the experimental set-up

Figure 5 presents a sketch of a cross sectional view of a model tower at the axis of the stack. Each 16-cell model tower was made up of four-stack towers. This was done to provide the flexibility required in the investigation of the effects of tower length and arrangement on recirculation and interference. Cooling-tower dimensions were obtained from drawing #4-68295 supplied by TVA. Each model cooling tower cell has one stack-effluent inlet and two intake ports (one each for the upstream and downstream faces of the tower); thus there were thirty-two stack-effluent inlets and sixty-four intake ports for the two 16-cell towers. It was considered to be impractical to meter the discharge through each effluent and each intake port separately. Instead, the four stack effluent inlet, the four upstream intake ports, and the four downstream intake ports for each model tower were each connected to a separate manifold (figure 6), and the discharge through each manifold was metered by means of a calibrated orifice meter and two-tube manometer. Effluent flows approached the model stacks through conical diffusers filled with rubberized hair, to produce smooth transitions and prevent separation and thereby assure that flows were well distributed over the stack cross-sections. The tower louver faces were simulated by means of perforated plates with a sufficiently small opening ratio that discharges through the louver faces were uniformly distributed. Water passing through the louver (intake) faces entered suction chambers from which it was withdrawn through intake ports installed in the floors of the towers. The withdrawn water was returned, after passing through manifolds, orifice meters, and the pump, to the downstream end of the EFF. A layer of polyurathane insulation was placed around the diffuser and stack efflux inlet upstream from each model stack, to reduce heat transfer between the louver-face flows and the stack flows.

Heated water was supplied to the stacks through two 500,000 Btu/hr (146.6 kw) gas fired water heaters; cold (ambient) water pumped to the heaters was withdrawn from the flume at a point near its downstream end. Temperature control of the effluent was accomplished by adjusting the supply of natural gas to the water heaters. Hot water from the heaters entered a large manifold from which it passed through valves, calibrated orifice meters, and small manifolds to the model cooling tower stacks. The hot water discharge to each small manifold was valve-controlled and metered. The water withdrawn through
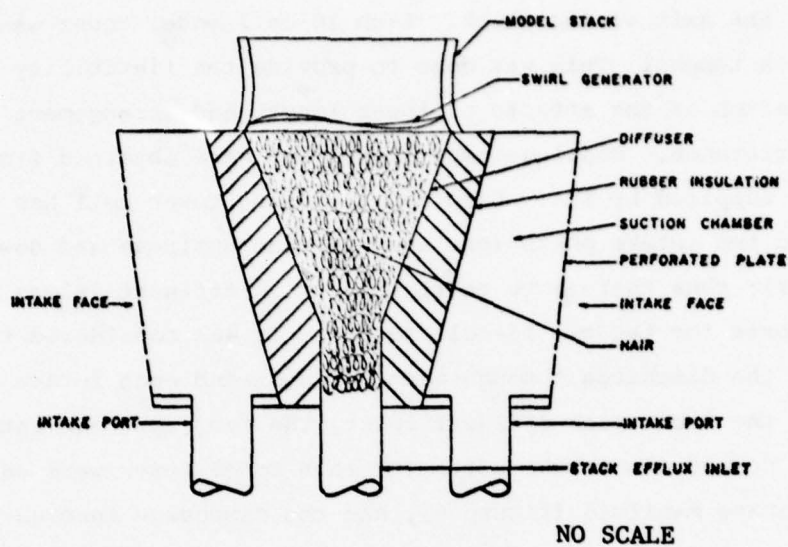
Figure 5. Details of cooling tower model construction
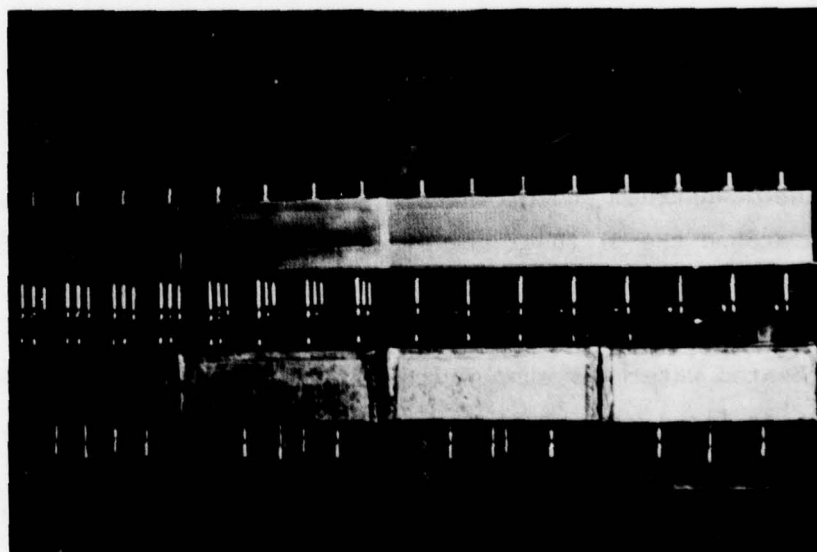
Figure 6. Photograph of the cooling tower model

the intake faces of the towers traveled through the intake ports and small manifolds into pipes fitted with valves and orifice meters, and then to a large manifold from which it was pumped to the downstream end of the flume. The discharge through small manifold connected to four intake ports of each tower segment was separately metered and adjusted such that the stack discharge equaled that through corresponding louver faces.

The temperature measuring system consisted of 35 thermistor probes which were capable of temperature resolution of 0.02°F over the range of calibration. One probe was positioned upstream from the towers and used to measure the ambient temperature, T_a; two probes were placed in heated effluent lines to measure the effluent temperature, T_j; one probe was installed in each withdrawl line to measure the temperature of the water withdrawn through the four section chambers to which it was connected, from which the amount of recirculation was determined for each tower segment; (as explained in the next section) and the remaining probes were mounted on a specially designed carriage and could be moved easily from one position to another to measure spatial distributions of the relative temperature-rise ratio, $\Delta T/\Delta T_o$, from which the plume configurations were determined. Each probe was interfaced through its own bridge circuit with the Institute's IBM 1800 Data Acquisition and Control System. The thermistors were calibrated in an insulated bath over a temperature range of 15°F, and the calibration relations so obtained were quantified by a least-square fit to a second-order polynomial and stored in the IBM 1800. The outputs from each thermistor bridge were processed by the computer, which averaged the voltage outputs over a period of several minutes, calculated the corresponding temperature using the stored calibration curves, and printed the bridge voltage and the normalized temperature-rise ratio, $\Delta T/\Delta T_o$ for each probe. The temperature measurements were judged to be accurate to $\pm$ 0.05°F.

Prior to each tests, the required values of effluent discharge through each stack, the rate of water withdrawal through each intake port, the ambient velocity, and the difference between the effluent and the ambient temperatures were calculated for the given prototype values of the densimetric Froude number, F_D, and the velocity ratio, K. Three principal adjustments were made for each experiment: (1) the valves in each discharge and withdrawal line were adjusted until the required stack and intake discharges were obtained;

(2) the gas flows to the water heaters were adjusted to obtain the desired temperature difference between the effluent and the ambient flows; and (3) the cross-flow velocity was adjusted, by varying the pump speed, adjusting the pump-intake valves, or both. After these adjustments were completed, the gas supply to the heaters was stopped so that all thermistors in the system were at the ambient temperature and a "zero temperature" data set was obtained. The "zero temperature" set was stored in the computer, and the difference between the temperature obtained from each thermistor and the measured ambient temperature was later used as a correction to the temperatures measured by the thermistor. The gas supply to the water heaters was then restored and temperature measurements were taken after steady conditions were attained. The temperatures and discharges were checked at frequent intervals. Photographs of the dyed plumes were obtained during most experiments.

V. EXPERIMENTAL RESULTS

A summary of experimental conditions is given in table 1, which also includes the prototype flow conditions from which the model flow conditions were determined according to the dynamic simularity principal developed in Section III: equality of the jet densimetric Froude number and of the velocity ratio in the model and prototype. Tests were conducted at F_D = 4.26 and K = 1,2 and 4, and at F_D = 5.68 and K = 2. The ambient wind velocity at the elevation of the tops of the stacks was used to determine the velocity ratio K. The measured normalized ambient-flow velocity distribution in the flume is shown in figure 7. It is seen to conform well to the 1/6-power law, which is known to be a good approximation for the velocity distribution in a neutral atmospheric boundary layer over rural terrain.

The recirculation ratio, R, was used as a quantitative measure of the tower performance. The recirculation ratio (which hereinafter includes the effects of interference) for any intake face of the cooling tower is defined as the fraction of stack effluent in the fluid withdrawn into that face of the tower. The value of R for any tower segment was calculated from the experimental results as

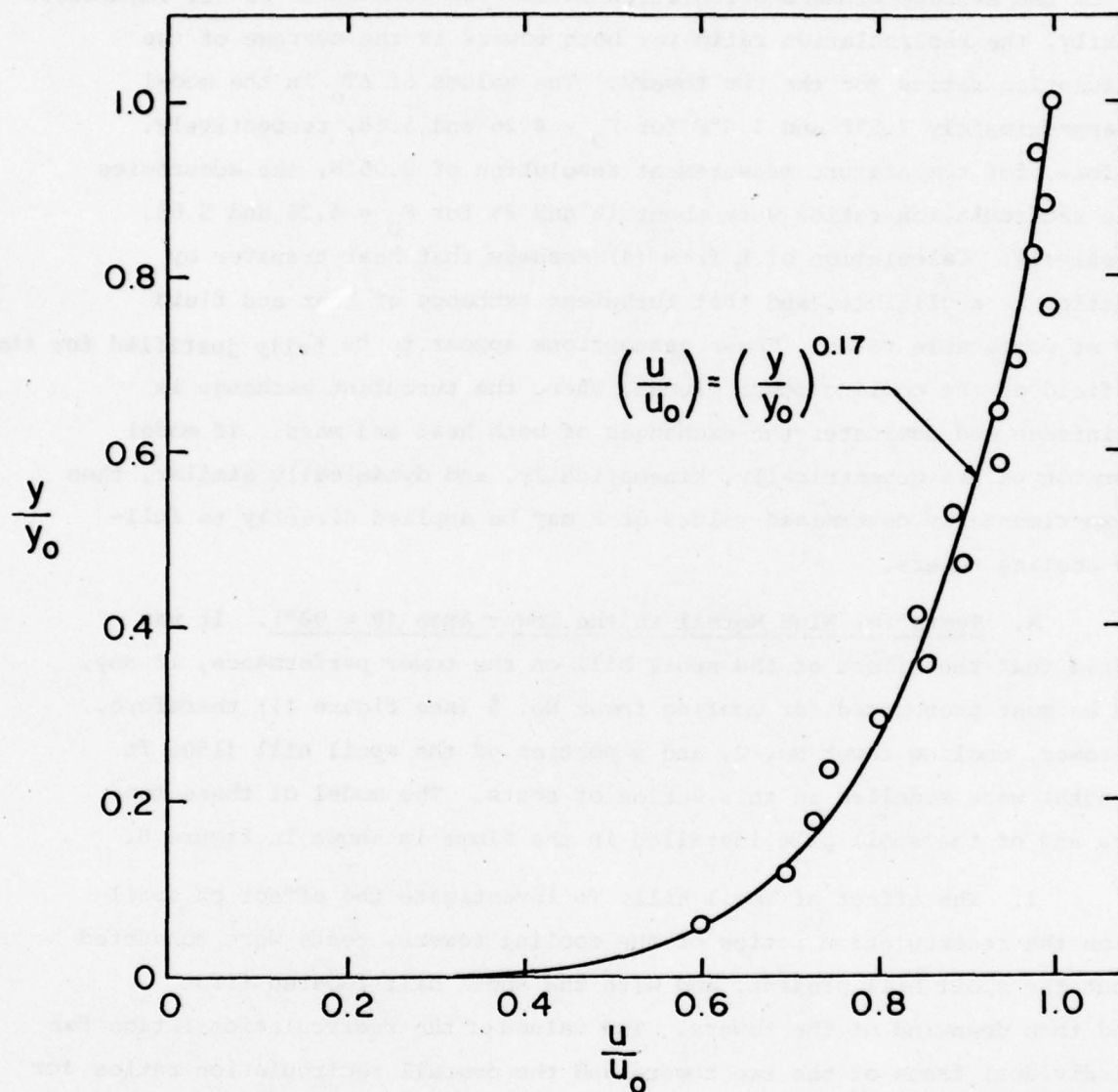$$R = \frac{\bar{T}_w - \bar{T}_a}{T_j - T_a} = \frac{\bar{\Delta T}_w}{\Delta T_o} \tag{4}$$

Figure 7. Measured normalized ambient velocity distribution
in the flume

where $\bar{T}_w$ is the average of the temperature measured in the individual intake manifolds and $\bar{\Delta T}_w = \bar{T}_w - T_a$. The recirculation ratio for a whole tower is the average of the recirculation ratios for both faces of all segments. Similarly, the recirculation ratio for both towers is the average of the recirculation ratios for the two towers. The values of ΔT_o in the model were approximately 7.5°F and 4.4°F for F_D = 4.26 and 5.68, respectively. Therefore, for temperature measurement resolution of 0.05°F, the accuracies of the recirculation ratios were about 1% and 2% for F_D = 4.26 and 5.68, respectively. Calculation of R from (4) assumes that heat transfer by conduction is negligible, and that turbulent exchange of heat and fluid occur at comparable rates. These assumptions appear to be fully justified for the near field of the cooling tower plumes, where the turbulent exchange is very intense and dominates the exchanges of both heat and mass. If model and prototype are geometrically, kinematically, and dynamically similar, then the experimentally determined values of R may be applied directly to full-scale cooling towers.

A. Tests for Wind Normal to the Tower Axes (θ = 90°). It was expected that the effect of the spoil hill on the tower performance, if any, would be most pronounced for cooling tower No. 5 (see figure 1); therefore, this tower, cooling tower No. 2, and a portion of the spoil hill (1500 ft in length) were modelled in this series of tests. The model of these two towers and of the spoil pile installed in the flume is shown in figure 8.

1. The effect of spoil hill. To investigate the effect of spoil hill on the recirculation ratios of the cooling towers, tests were conducted without the spoil hill present, and with the spoil hill located first upwind then downwind of the towers. The values of the recirculation ratios for the individual faces of the two towers and the overall recirculation ratios for both towers, $\bar{R}$, are given in table 2(a). The recirculation ratio for the upwind face of the upwind tower, R_{uu}, was, of course, zero in all the tests. The variation of the overall recirculation ratio, $\bar{R}$, with velocity ratio, K, is shown in figure 9 for F_D = 4.26. The value of $\bar{R}$ decreases with increasing K and with the decrease in F_D, as one would expect. The effect, if any, of spoil hill on $\bar{R}$ is seen to be so small as to be practicaly within the limits of experimental resolution of $\bar{R}$. Moreover, this finding is consistent with
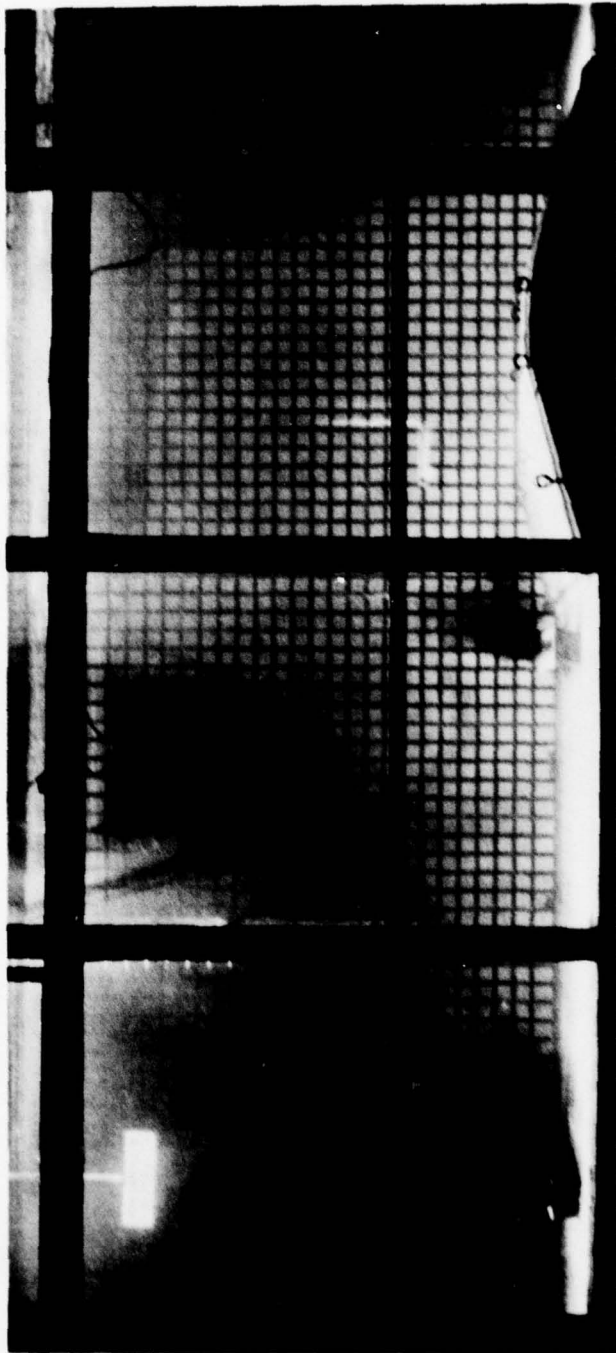
Figure 8. Cooling towers and spoil hill installed in the flume

Table 1. Prototype and Model Test Conditions

	Prototype	Model
Stack diameter at fan elevation (ft)	28.0	0.187
Exit velocity at fan elevation (fps)	35.0	0.311
Exit wet-bulb temperature (°F)	104.0	–
Approach (°F) for a design wet-bulb temperature of 55°F	29.0	–
Corresponding Range (°F)	31.7	–
Normalized density deficiency, $\Delta\rho_o/\rho_a$		
a) at full-plant load	0.075	8.83×10^{-4}
b) at 65% of the plant load	0.042	4.97×10^{-4}
Jet densimetric Froude number		
a) at full plant load	4.26	4.26
b) at 65% of the plant load	5.68	5.68
Ambient flow velocity, V_a (fps)		
a) K = 1	35.0	0.311
b) K = 2	17.5	0.155
c) K = 4	8.75	0.078

Table 2. Data Summary for Recirculation Tests ($\theta = 90°$)

F_D	K	Spoil hill location	R_{ud}^1 %	R_{du}^2 %	R_{dd}^3 %	$\bar{R}^4$ %
			a. Without any tower modification			
4.26	1	w/o[5]	19.9	7.3	27.1	13.6
4.26	2	w/o	17.1	5.0	21.1	10.8
4.26	4	w/o	7.8	0.3	6.8	3.7
5.68	2	w/o[6]	20.0	6.9	24.4	12.8
4.26	1	u/w	21.8	7.3	27.9	14.2
4.26	2	u/w	15.7	4.4	19.6	9.9
4.26	4	u/w	8.2	0.0	6.5	3.7
5.68	2	u/w[7]	19.3	7.5	22.4	12.3
4.26	1	d/w	20.2	6.2	27.2	13.4
4.26	2	d/w	18.8	4.5	15.1	9.6
4.26	4	d/w	7.0	0.0	2.3	2.3
5.68	2	d/w	18.5	7.3	22.3	12.0
			b. With 72-foot spacing in the center of the towers			
4.26	1	w/o	21.1	7.6	24.4	13.3
4.26	2	w/o	16.6	6.6	20.5	10.9
4.26	4	w/o	9.2	0.7	10.3	5.1
5.68	2	w/o	18.5	9.7	23.3	12.9
4.26	1	u/w	21.3	6.8	22.8	12.7
4.26	2	u/w	15.2	5.8	19.0	10.0
4.26	4	u/w	9.7	2.7	11.3	5.9
5.68	2	u/w	16.0	9.5	20.4	11.5
4.26	1	d/w	18.9	5.7	21.9	11.6
4.26	2	d/w	14.3	4.9	16.8	9.0
4.26	4	d/w	8.7	0.0	5.9	3.7
5.68	2	d/w	15.0	5.9	18.1	9.8
			c. With stack height of 42 ft			
4.26	1	D/W	12.6	6.6	15.9	8.8
4.26	2	D/W	9.7	4.1	11.0	6.2
4.26	4	D/W	7.0	1.8	3.8	3.2
5.68	2	D/W	11.8	6.7	13.2	7.9

1   R_{ud} = Recirculation ratio for the d/w face of the u/w tower

2   R_{du} = Recirculation ratio for the u/w face of the d/w tower

3   R_{dd} = Recirculation ratio for the d/w face of the d/w tower

4   $\bar{R}$ = Overall recirculation ratio for both towers

5   w/o = without spoil hill

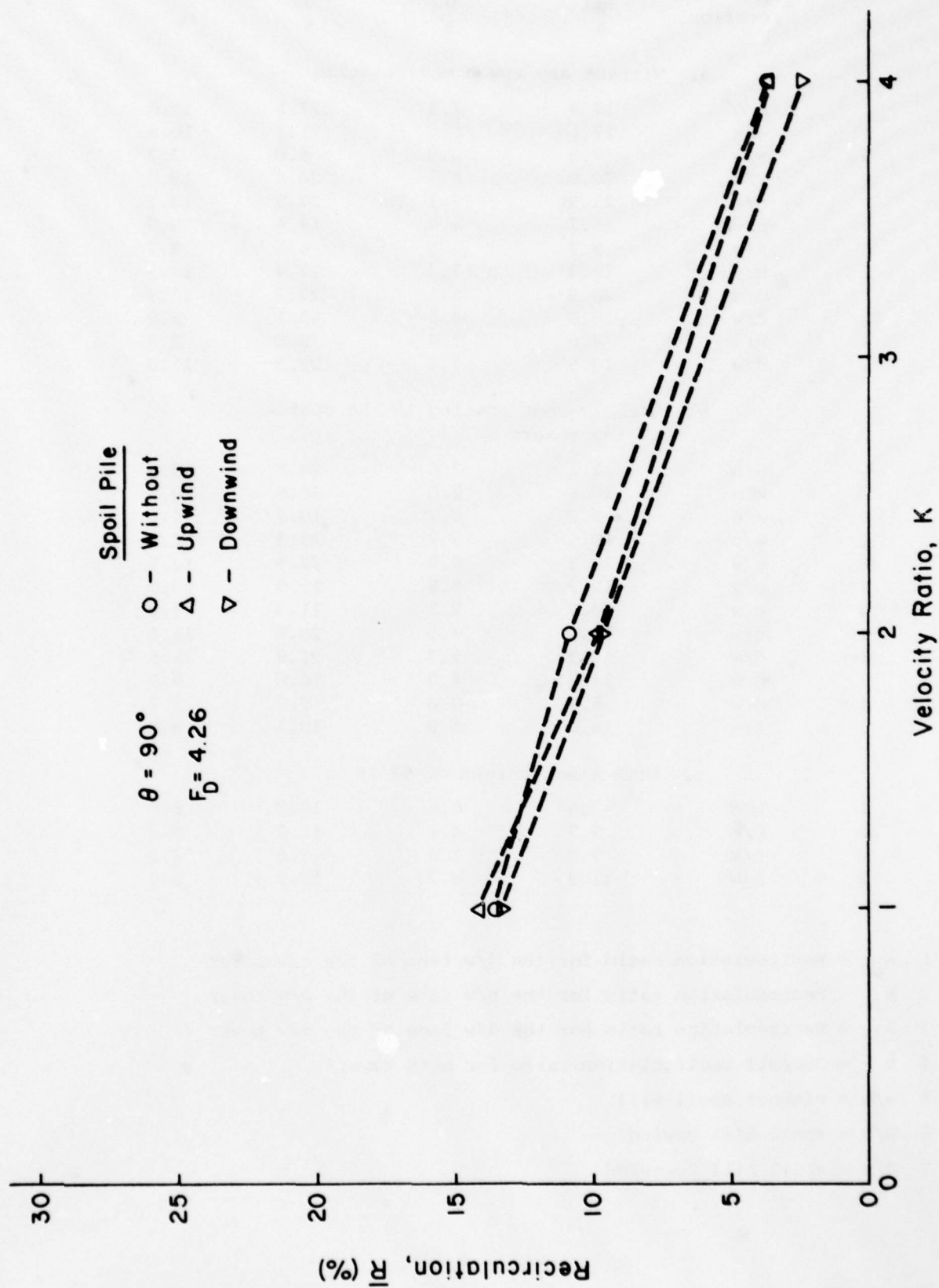6   u/w = spoil hill upwind

7   d/w = spoil hill downwind

Figure 9. Effect of spil hill on recirculation ratio

visual observations made in the course of the tests. Although the presence of the spoil hill affected the flow near it, it produced no observable effect on the interaction between the deflected plume and the tower wake.

2. The effect of cell arrangement. A spacing of 72 ft (which is equal to the length of two cells) was provided between 8th and 9th cells of both towers to permit ambient flow through the center of the towers and thereby provide better ventilation of the downward faces of the towers. The array was then composed of four towers of 8 cells each, with a spacing of 72 ft (prototype) between adjacent towers. This could be achieved in prototype by removing two cells (say cells 9 and 10) and placing them adjacent to cell 16.

The model results are summarized in table 2(b). The variation of overall recirculation $\bar{R}$ with K is shown in figure 10, and is seen to be practically identical with that shown in figure 9. The recirculation ratios with spacing between the towers do not significantly differ from those of the longer towers. The values for the former are a little smaller for K=1, almost equal for K=2, and slightly higher for K=4 (recall here that the accuracy of recirculation measurements for K=4 is relatively poor, due to low values of $\bar{R}$). The effect of spoil hill on $\bar{R}$ is again seen to be small. Therefore, all subsequent tests with wind normal to the tower axes ($\theta = 90°$) were conducted with spoil hill downwind of the towers only.

3. The effect of stack height. The stack height was increased to 42 ft (prototype) from the existing 14 ft. The values of the recirculation ratio are given in table 2(c). The overall recirculation Ratio, $\bar{R}$, for various values of K is plotted in figure 11, which, for comparison, also includes the variation of $\bar{R}$ for other selected test conditions. Examination of the points labeled 3-D show that the increase in stack height significantly reduces the recirculation ratio for K=1 and 2, but has little if any effect on $\bar{R}$ at K=4. However, at the highest K the difference is within the experimental accuracy, and the recirculation is already relatively small.

4. The effect of tower length. These tests were conducted to determine the upper bound of the recirculation ratio which would occur for an infinitely long tower; i.e., for a two-dimensional (2-D) tower. The results of these tests will be useful in assessing the effect of adding cells to the existing towers. False walls parallel to the flow and adjacent

Table 3. Data Summary for Two-dimensional
Recirculation Tests ($\theta = 90°$; spoil
hill downwind)

A. Stack Height = 14 ft

F_D	K	R_{ud}	R_{du}	R_{dd}	$\bar{R}$
4.26	1	18.8	16.8	31.8	16.8
4.26	2	17.8	20.7	33.4	18.0
4.26	4	17.9	18.9	32.4	17.3
5.68	2	19.9	19.4	34.5	18.4

B. Stack Height = 42 ft

F_D	K	R_{ud}	R_{du}	R_{dd}	$\bar{R}$
4.26	1	9.1	16.3	22.5	12.0
4.26	2	9.2	19.2	25.8	13.6
4.26	4	8.1	7.7	18.1	8.9
5.68	2	9.5	22.3	27.3	14.8

Table 4. Data Summary of Recirculation Tests
($\theta = 45°$, stack height = 14')

F_D	K	Spoil hill location	R_{ud} %	R_{du} %	R_{dd} %	$\bar{R}$ %
4.26	1	w/o	29.2	7.4	33.3	17.5
4.26	2	w/o	16.9	4.0	11.9	8.2
4.26	4	w/o	5.1	0.6	0.3	1.5
5.68	2	w/o	17.5	7.9	22.1	11.9
4.26	1	u/w	26.5	7.3	32.3	16.5
4.26	2	u/w	13.5	4.2	11.9	7.4
4.26	4	u/w	5.9	0.1	0.2	1.6
5.68	2	u/w	14.5	7.1	20.8	10.6
4.26	1	d/w	27.8	6.7	28.1	16.6
4.26	4	d/w	6.6	0.2	0.4	1.8
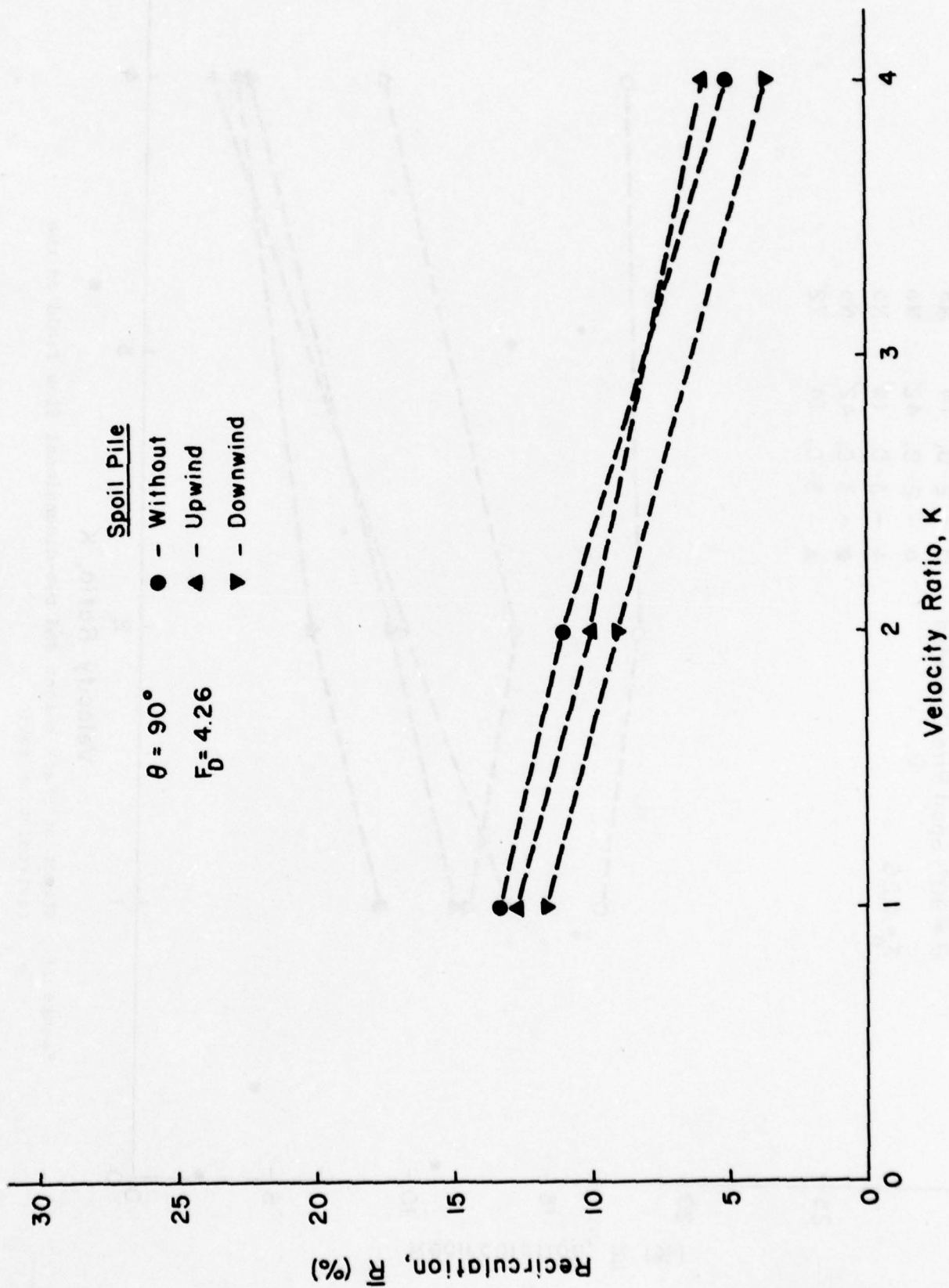
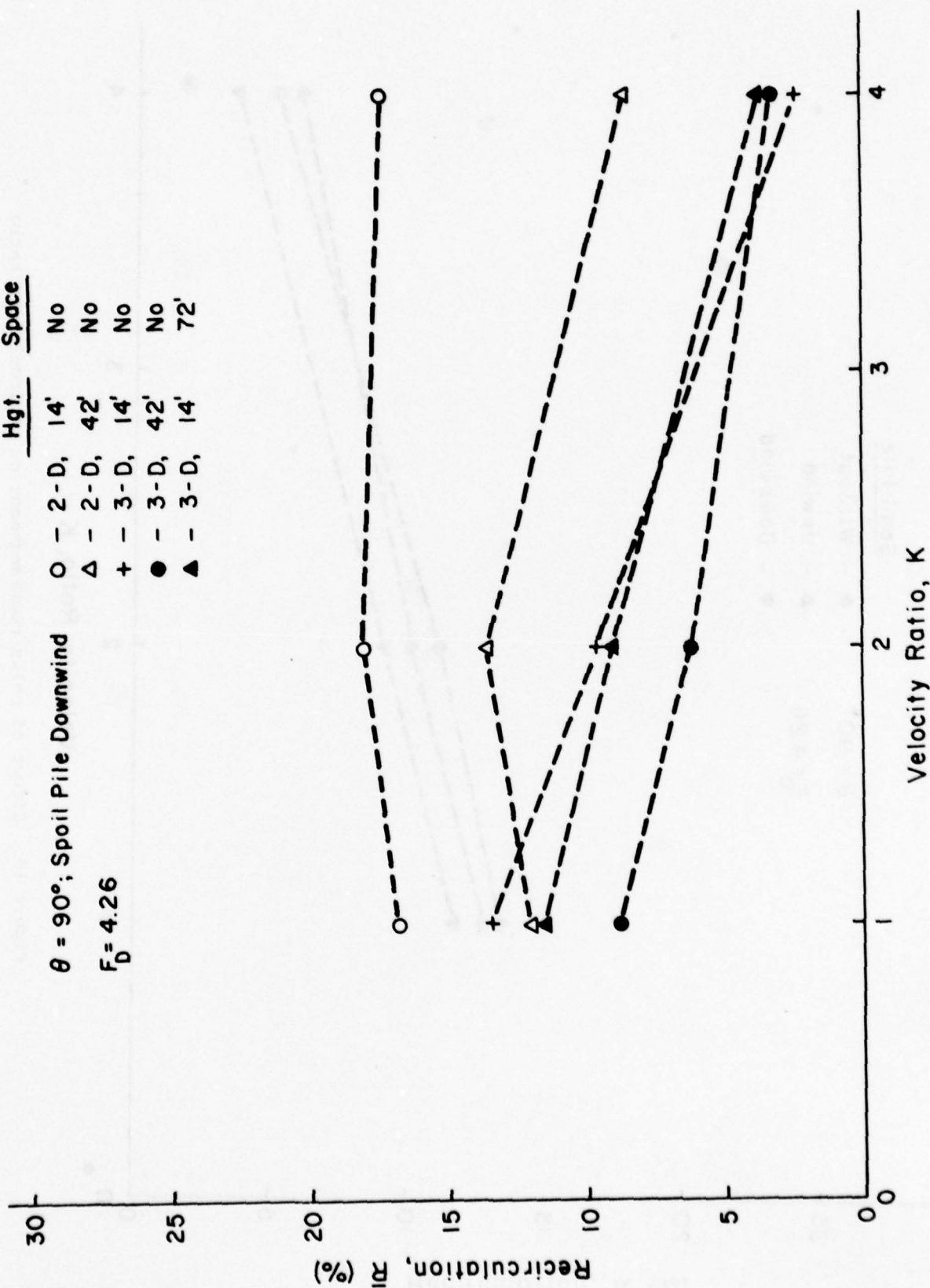Figure 10. Effect of cells rearrangement on recirculation ratio

Figure 11. Effect of stack height and two-dimensional flow field on the recirculation ratio

to the tower ends were installed, so that the effective width of the flume
was equal to the length of the tower. Tests were conducted with both the
42-ft and 14-ft high stacks. The experimental results are summarized in table 3,
and the overall recirculation ratios for various K values are plotted in
figure 11. The recirculation ratio $\bar{R}$ for an infinitely long tower (two-
dimensional: 2-D) is much higher than that for the shorter tower (three-
dimensional: 3-D). It is seen that the present tower configuration draws
a considerable amount of ambient flow around the ends of the towers. Morever, the
recirculation ratio for the two-dimensional case increases with K,
because the ambient flow available for diluting the stack effluent *decreases*
with increasing K. The taller stacks yielded considerable less recirculation
for two-dimensional case also.

B. Tests for Wind at $\theta = 45°$ to the Tower Axes ($\theta = 45°$). Cooling
towers Nos. 3 and 5, and the downwind (or upwind) portion of the spoil hill
were modelled in these tests. The cooling tower models were rotated so that
the tower axes were inclined to the flow direction. The values of the
recirculation ratio are given in table 4 and the experimental results are
plotted in figure 12. A comparison of $\bar{R}$ for $\theta = 90°$ and $\theta \approx 45°$ shows that
$\bar{R}$ for K=1, $\theta = 45°$ is higher than that for $\theta = 90°$, but at K=2 and 4, $\bar{R}$ is
lower for $\theta = 45°$. The effect of spoil hill is negligible for this wind
direction also.

C. Some Additional Results. In some of the early tests on the
existing tower configuration at $\theta = 90°$, temperature distributions at three
elevations (7 ft, 21 ft, and 35 ft) above the tower floor near the intake
faces of the tower were also measured. These data were intended for use in
validating the model results if corresponding prototype-measurement data
are obtained in the future. These results for $F_D = 4.26$, K = 1 and 2, and
spoil hill upwind and downwind of the tower are included in the Appendix
(figures A.1 through A.12). The data points in these figures represent the
percentage normalized temperature rise ($T^* = \dfrac{T-T_a}{T_j-T_a} \times 100$).

In some tests the cross-sectional temperature distributions in the
plume at two downwind sections, one about 550 feet downwind of the downwind
tower (location of the peak of the spoil hill) and without the spoil hill, and
the other 1000 feet downwind of the downwind tower, and with the spoil hill
downwind of the towers, were also measured. These measurements were required
to evaluate the fogging potentials. The results are shown in figures A.13
through A.19 of the Appendix.
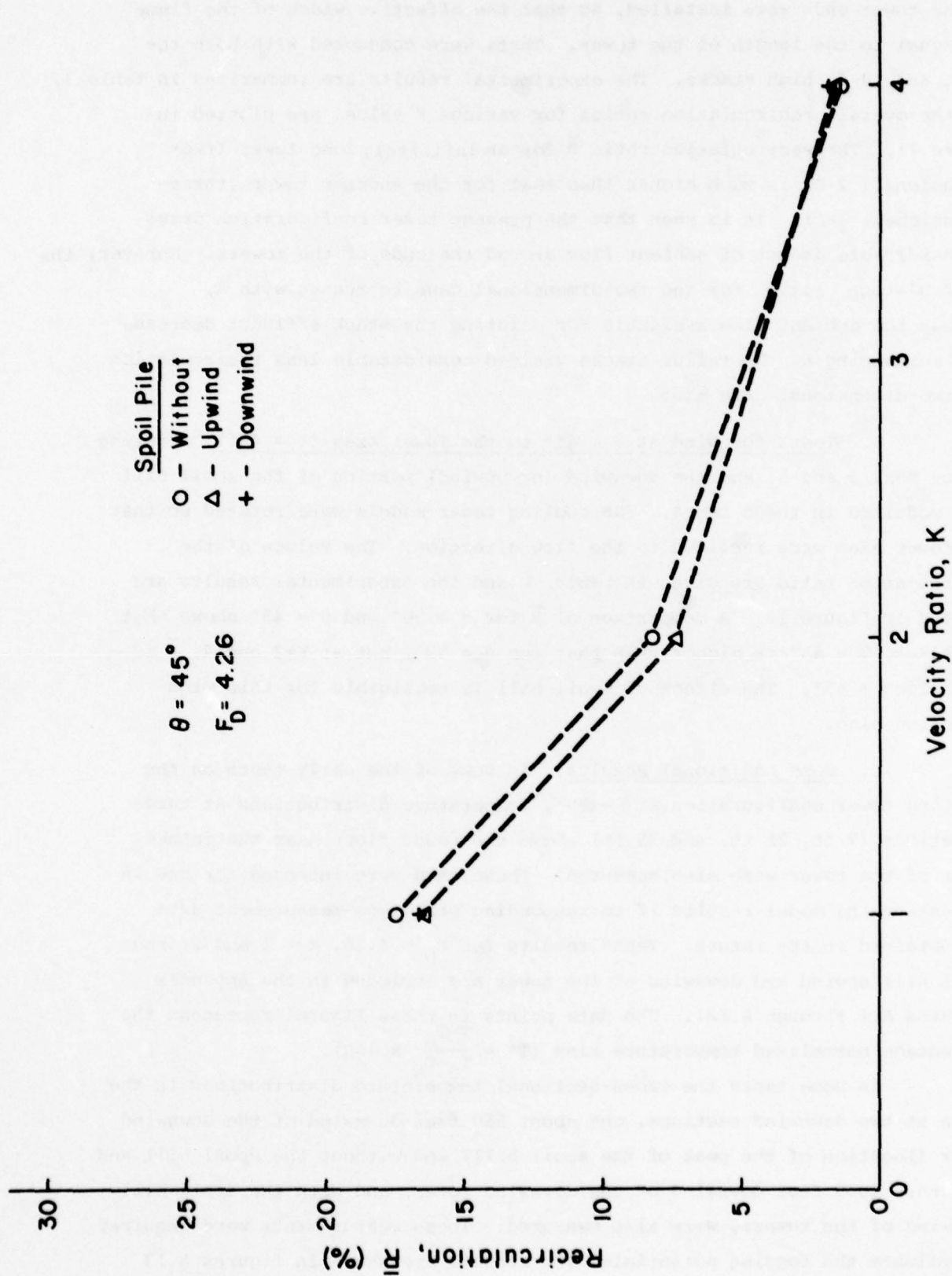
Figure 12. Recirculation ratio for θ = 45°

VI. SUMMARY OF RESULTS

The value of the overall recirculation, $\bar{R}$, decreases with increasing velocity ratio, K, and with decreasing densimetric Froude number, F_D, as one would expect. The observed values of $\bar{R}$ for the existing tower configuration with the spoil hill downward of the towers are:

F_D	θ	K	$\bar{R}(\%)$
4.26	90°	1	13.4
		2	9.6
		4	2.3
	45°	1	16.6
		2	7.8
		4	1.8
5.68	90°	2	12.0

The values of $\bar{R}$ with spoil hill upwind of the tower are within about ± 1% of the values given in the above table.

The effect on tower performance of some of the modifications tested are as follows:

1. The influence of the spoil hill on $\bar{R}$ is insignificant, amounting to no more than ± 1%.

2. The provision of 72-foot long openings at the centers of the towers, by relocating two cells per tower, to permit ambient flow around the ends of the resulting shortened towers, inappreciably reduced $\bar{R}$, by about 1.8% and 0.6% for K = 1 and 2, respectively.

3. An increase in stack height from 14 ft to 42 ft significantly reduced the tower recirculation, by about 4.6%, and 3.4% for K = 1 and 2, respectively.

4. The recirculation ratio for the existing tower is smaller than that of an infinitely long tower. The existing towers are, therefore, drawing significant amounts of ambient fluid around the tower ends.

References

1. Chan, T.-L., Hsu, S.-T., Lin, J.-T., Hsu, K.-H., Huang, N.-S., Jain, D.C., Tsai, C.E., Croley, T.E., Fordyce H., and Kennedy, J.F., "Plume Recirculation and Interference in Mechanical Draft Cooling Towers", IIHR Report No. 160, Institute of Hydraulic Research, The University of Iowa, Iowa City, Iowa, April 1974.

2. Counihan, J., "An Improved Method of Simulating an Atmospheric Boundary Layer in a Wind Tunnel", Atmospheric Environment, Peragamon Press 1969, Vol. 3.

3. Waldrop, W.R., Almquist, C.W., Harper, W.L., Stubblefield, D., and Ungate, C.D., "Hydrothermal Analysis of Helper and Open Mode Condenser Cooling at the Browns Ferry Nuclear Plant", Report No. 63-66, Water Systems Development Branch, TVA, Norris, Tennessee, July 1977.

APPENDIX

$F_D = 4.26$

582'

14' 14' 7'

15 23 23 22 22 22 23 21 21 22 22 23 22 23 22 16

10 23 23 24 24 23 22 22 22 22 22 23 23 23 23 19 9

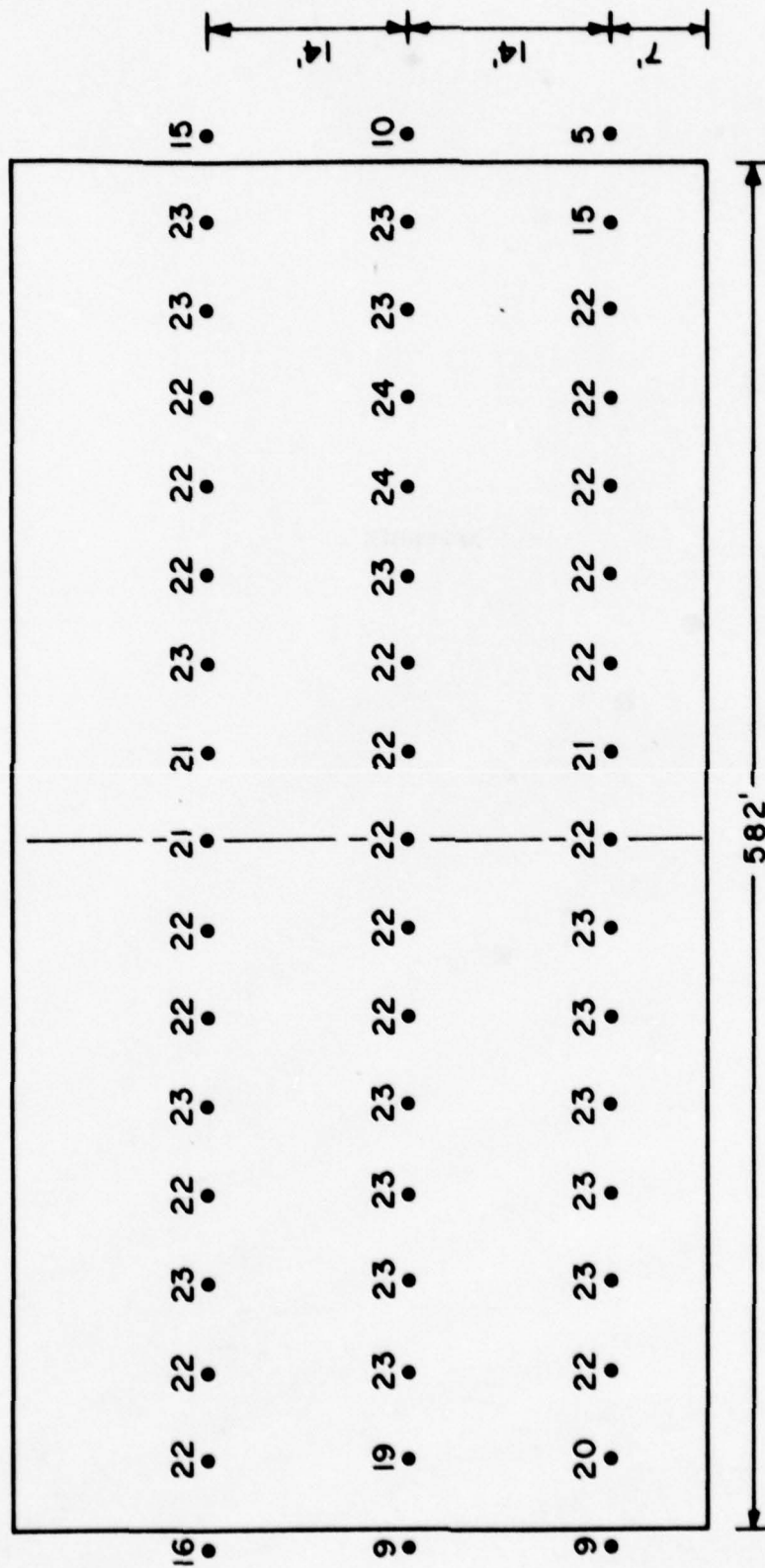5 15 22 22 22 22 22 21 22 23 23 23 23 23 22 20 9

Figure A.1 Percentage normalized temperature rise distribution near downwind face of the upwind tower with the spoill hill downwind of the towers and for K=1
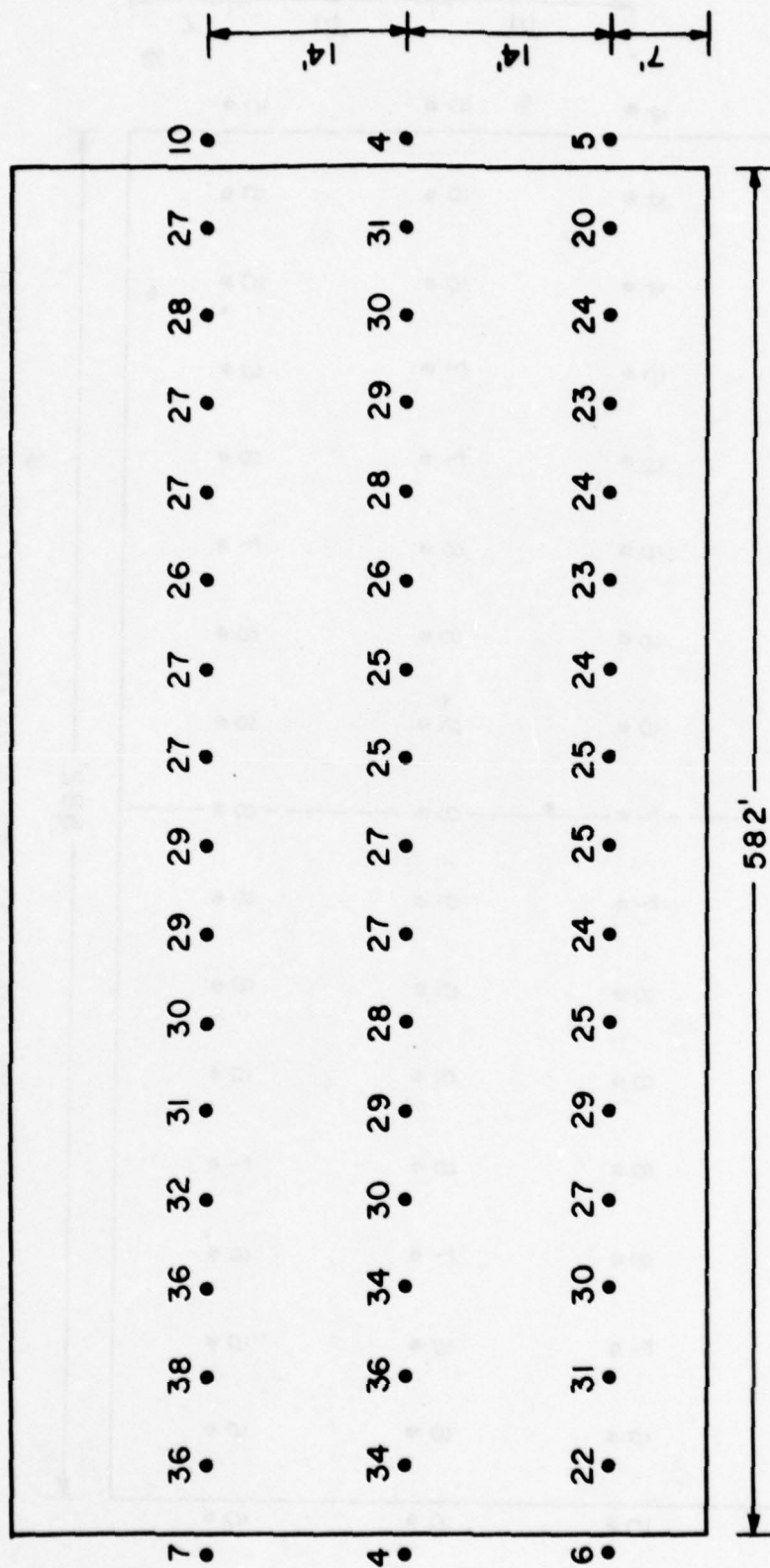
Figure A.2 Percentage normalized temperature rise distribution near upwind face of the downwind tower with the spoil hill downwind of the towers and for K=1

$F_D = 4.26$

7 •   36 •   38 •   36 •   32 •   31 •   30 •   29 •   29 •   27 •   27 •   26 •   27 •   27 •   28 •   27 •   10 •

4 •   34 •   36 •   34 •   30 •   29 •   28 •   27 •   27 •   25 •   25 •   26 •   28 •   29 •   30 •   31 •   4 •

6 •   22 •   31 •   30 •   27 •   29 •   25 •   24 •   25 •   25 •   24 •   23 •   24 •   23 •   24 •   20 •   5 •

582'

14'   14'   7'

Figure A.3   Percentage normalized temperature rise distribution near downwind face of the downwind tower with the spoil hill downwind of the towers and for K=1
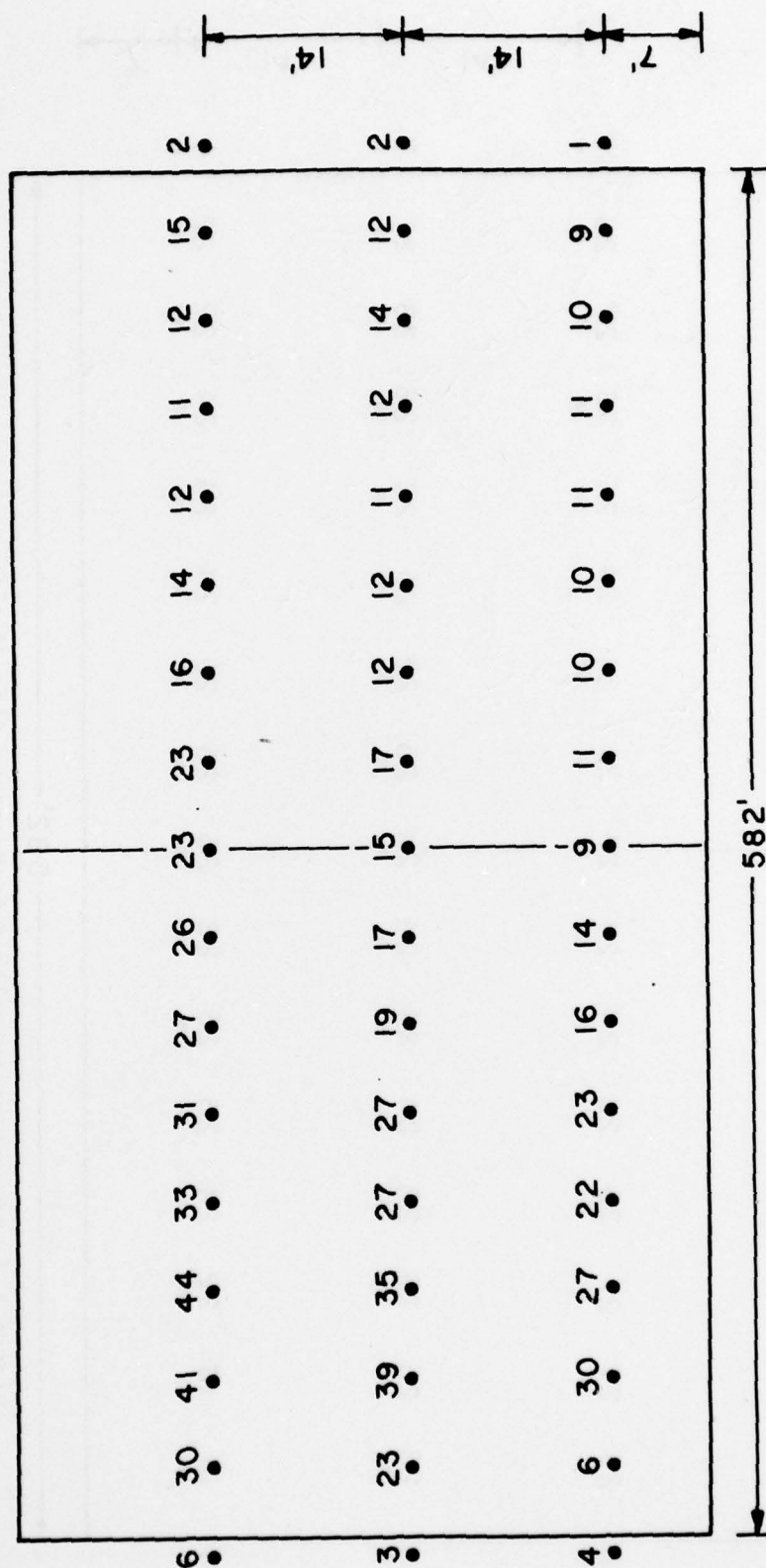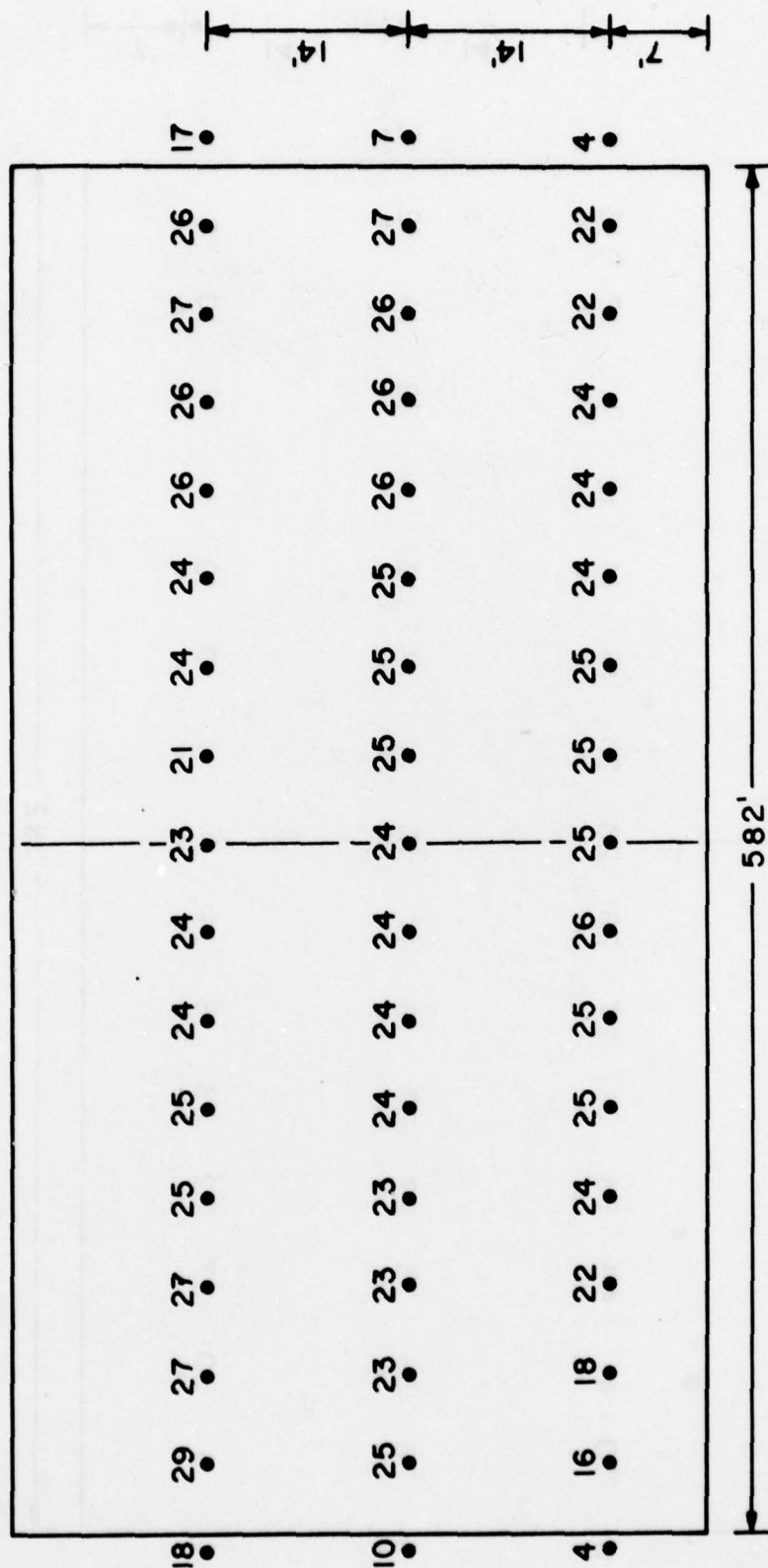
$F_D = 4.26$

6	14	15	16	16	17	17	19	15	17	19	20	20	21	21	23	11

Figure A.4 Percentage normalized temperature rise distribution near downwind face of the upwind tower with the spoil hill downwind of the towers and for K=2
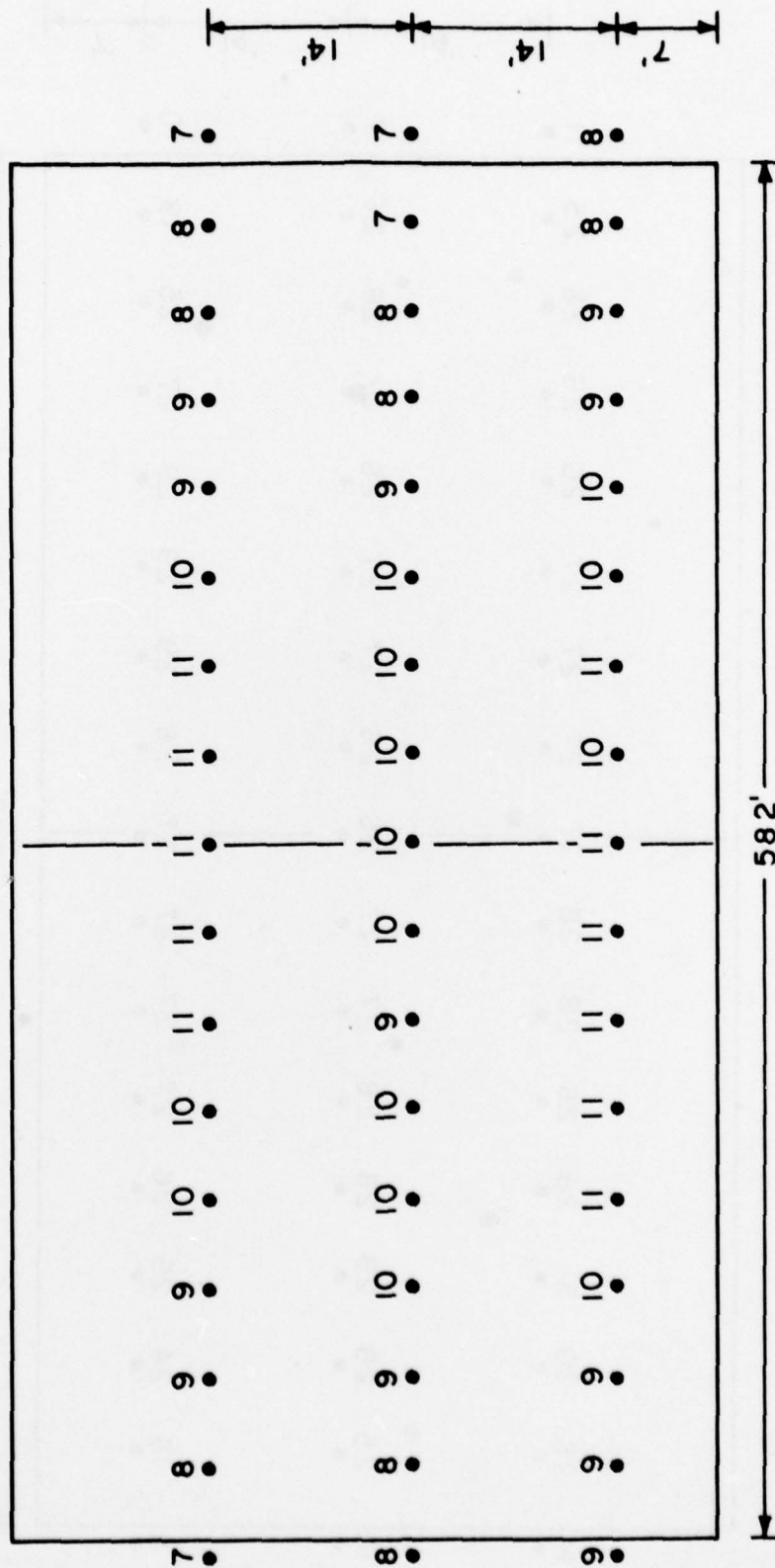
$F_D = 4.26$

582'

Figure A.5 Percentage normalized temperature rise distribution near upwind face of the downwind tower with the spoill hill downwind of the towers and for K=2
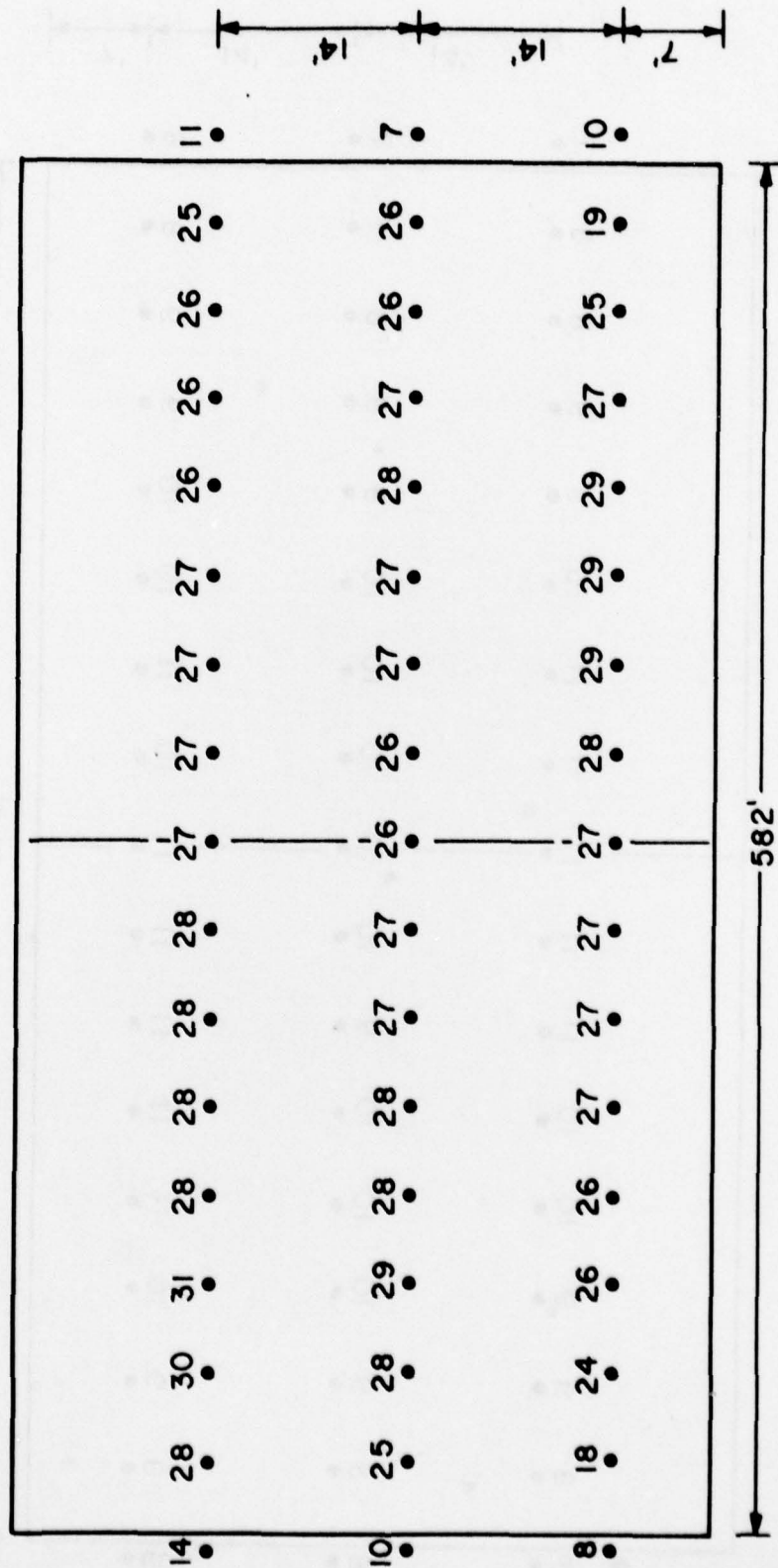
Figure A.6 Percentage normalized temperature rise distribution near downwind face of the downwind tower with the spoil hill downwind of the towers and for K=2

$F_D = 4.26$

582'

14' 14' 7'

Row 1: 18 29 27 27 25 24 25 24 23 21 24 24 26 26 27 26 17

Row 2: 10 25 23 23 25 23 24 24 25 25 25 25 26 26 27 27 7

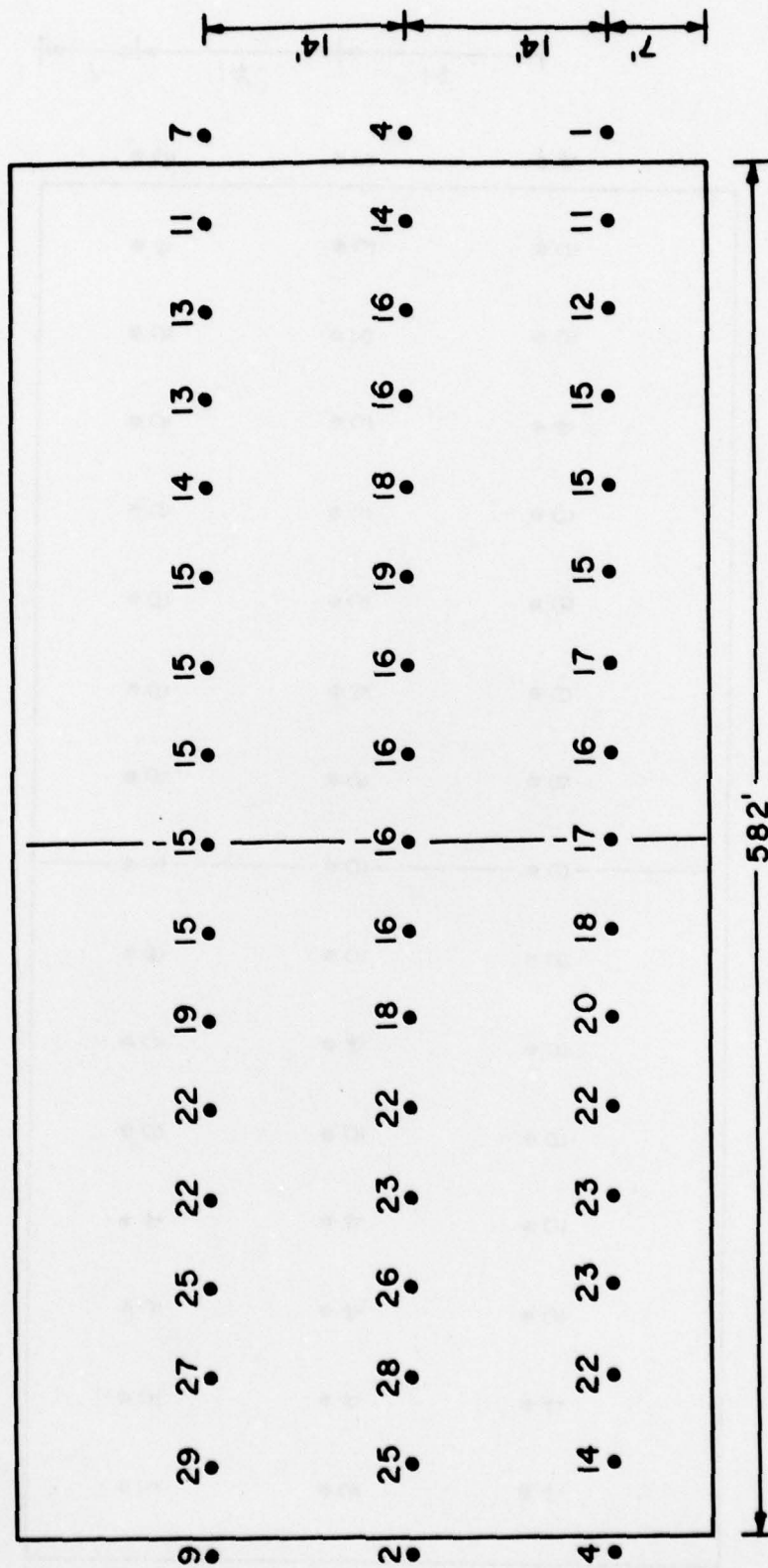Row 3: 4 16 18 22 24 25 25 25 24 24 24 24 24 22 22 4

Figure A.7 Percentage normalized temperature rise distribution near downwind face of the upwind tower with the spoil hill upwind of the towers and for K=1
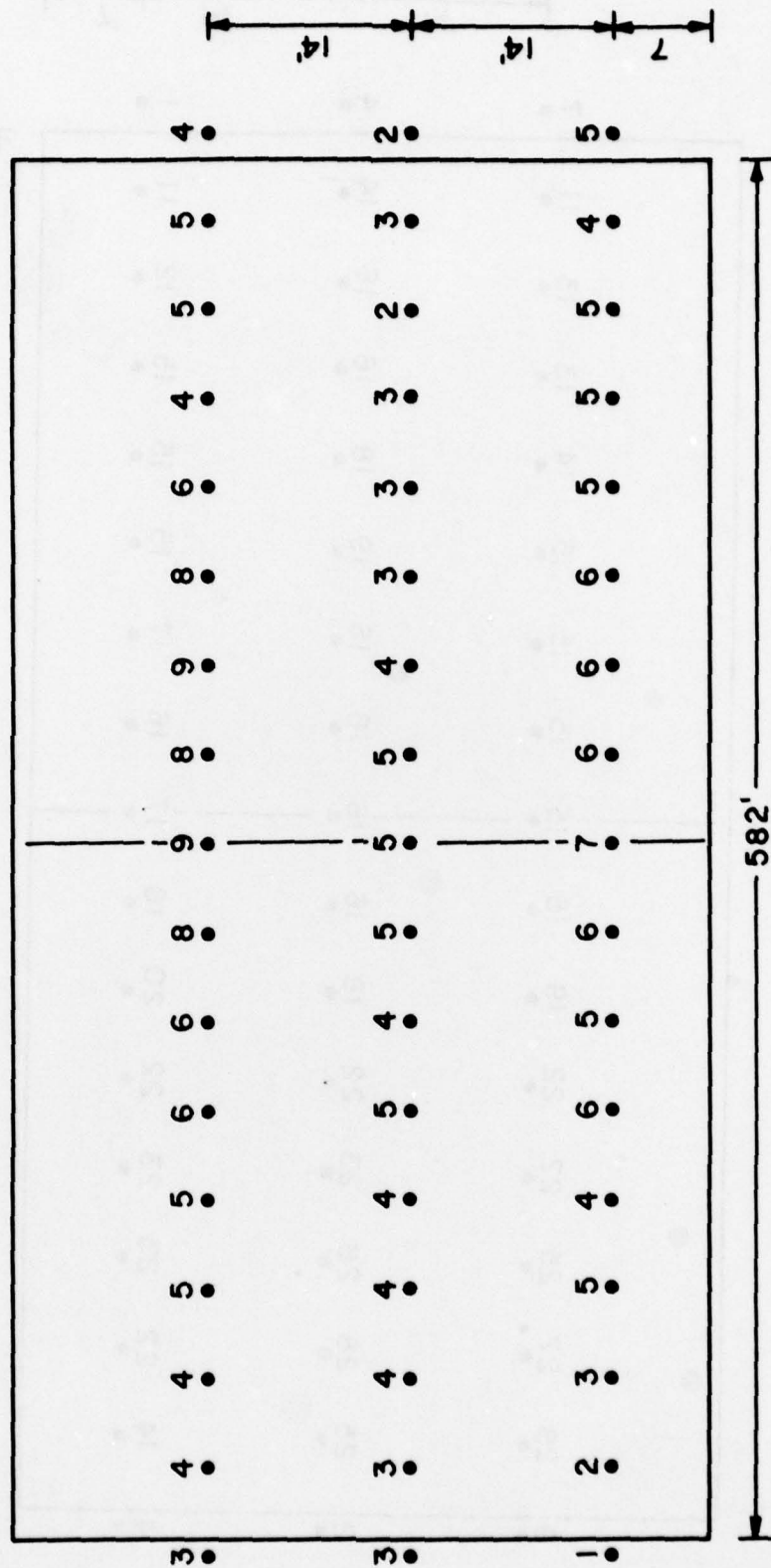
Figure A.8 Percentage normalized temperature rise distribution near upwind face of the downwind tower with the spoil hill upwind of the towers and for K=1

$F_D = 4.26$

582'

14' 14' 7'

11 25 26 26 26 27 27 27 27 28 28 28 28 31 30 28 14

7 26 26 27 28 27 27 26 26 27 27 28 28 29 28 25 10
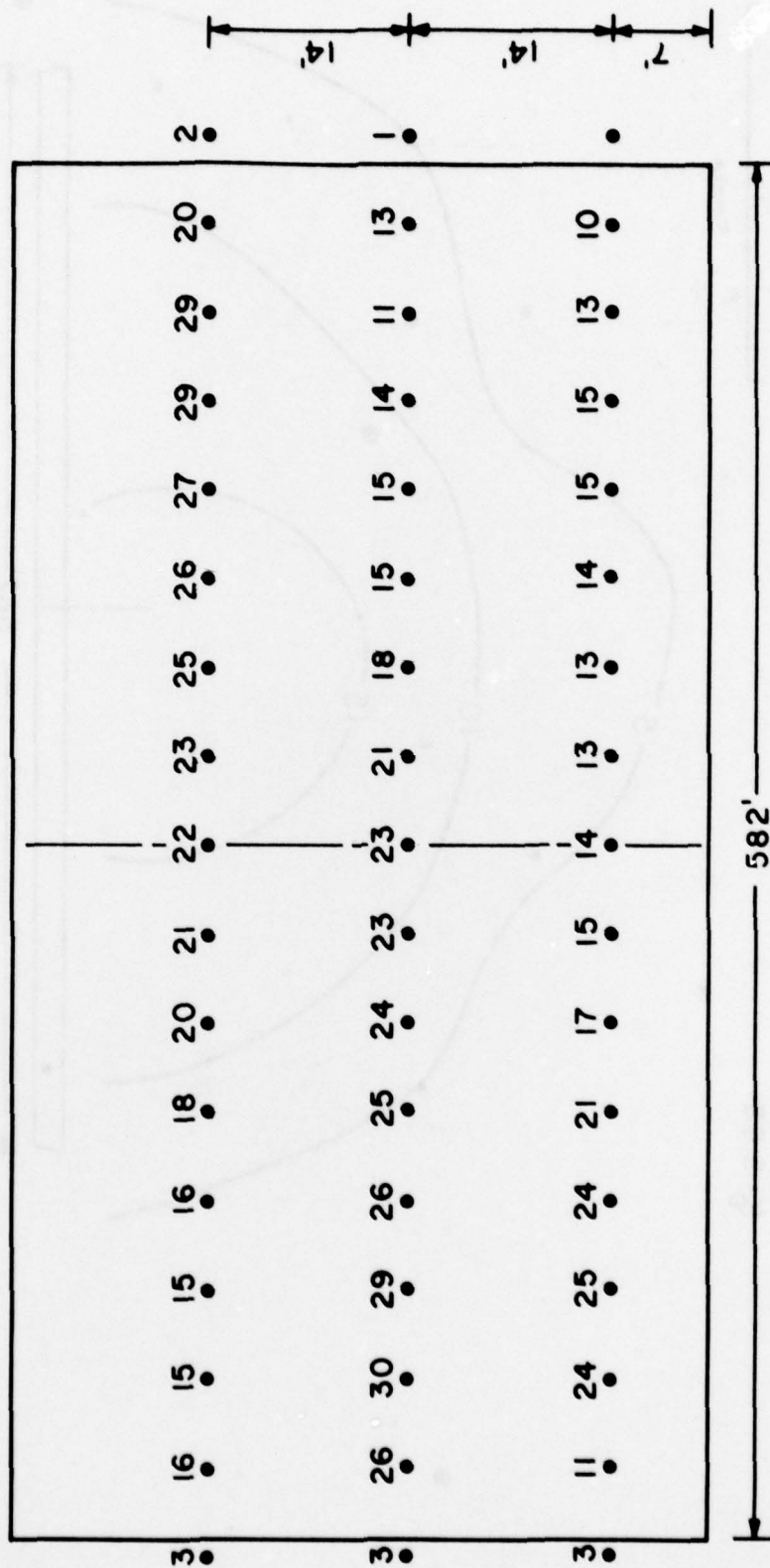
10 19 25 27 29 29 29 28 27 27 27 27 26 26 24 18 8

Figure A.9 Percentage normalized temperature rise distribution near downwind face of the downwind tower with the spoil hill upwind of the towers and for K=1

$F_D = 4.26$

14' 14' 7'

582'

Figure A.10 Percentage normalized temperature rise distribution near downwind face of the upwind tower with the spoil hill upwind of the towers and for K=2

Row 1: 7 11 13 13 14 15 15 15 15 15 19 22 22 25 27 29 9

Row 2: 4 14 16 16 18 19 16 16 16 16 18 18 22 23 26 28 25 2

Row 3: 1 11 12 15 15 15 17 16 17 18 20 22 23 23 22 14 4

$F_D = 4.26$

582'

14' 14' 7'

Figure A.11 Percentage normalized temperature rise distribution near upwind face of the downwind tower with the spoil hill upwind of the towers and for K=2

$F_D = 4.26$

Figure A.12 Percentage normalized temperature rise distribution near downwind face of the downwind tower with the spoil hill upwind of the towers and for K=2
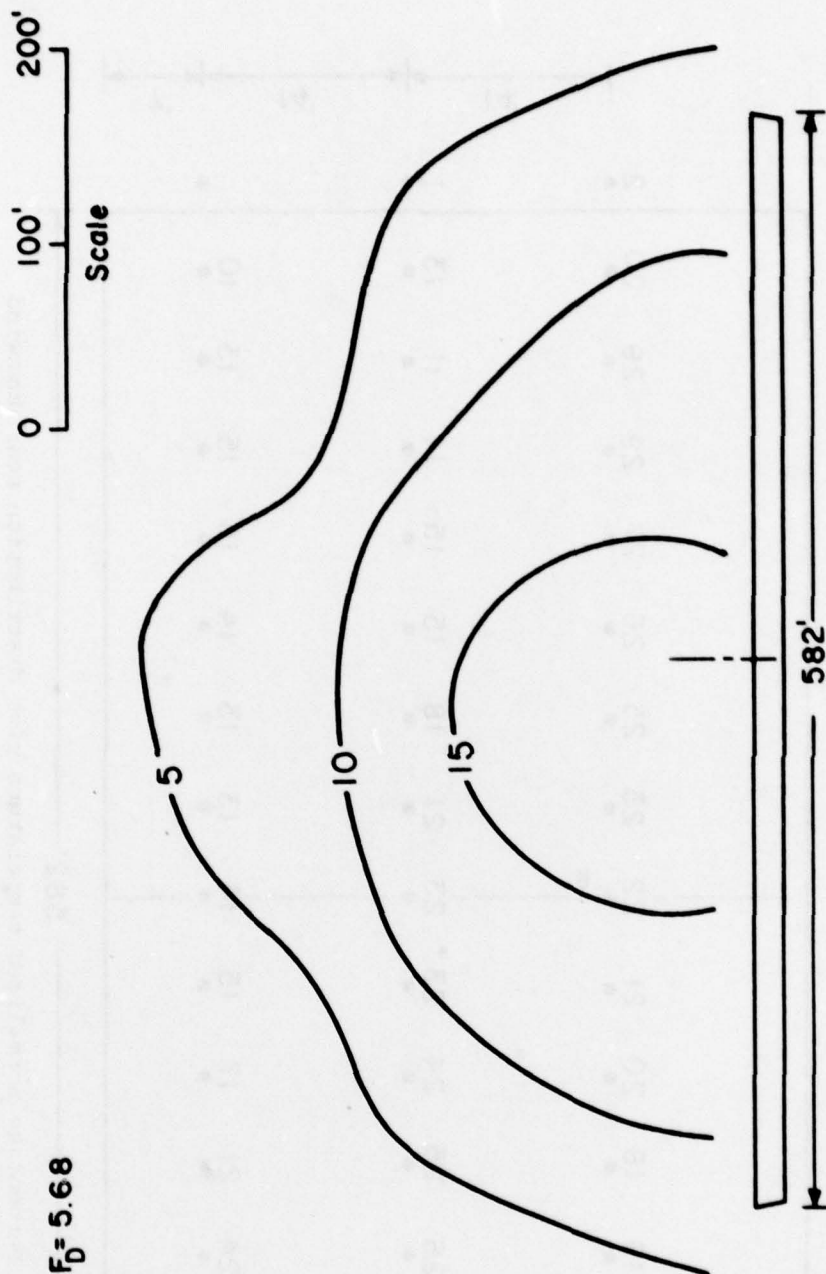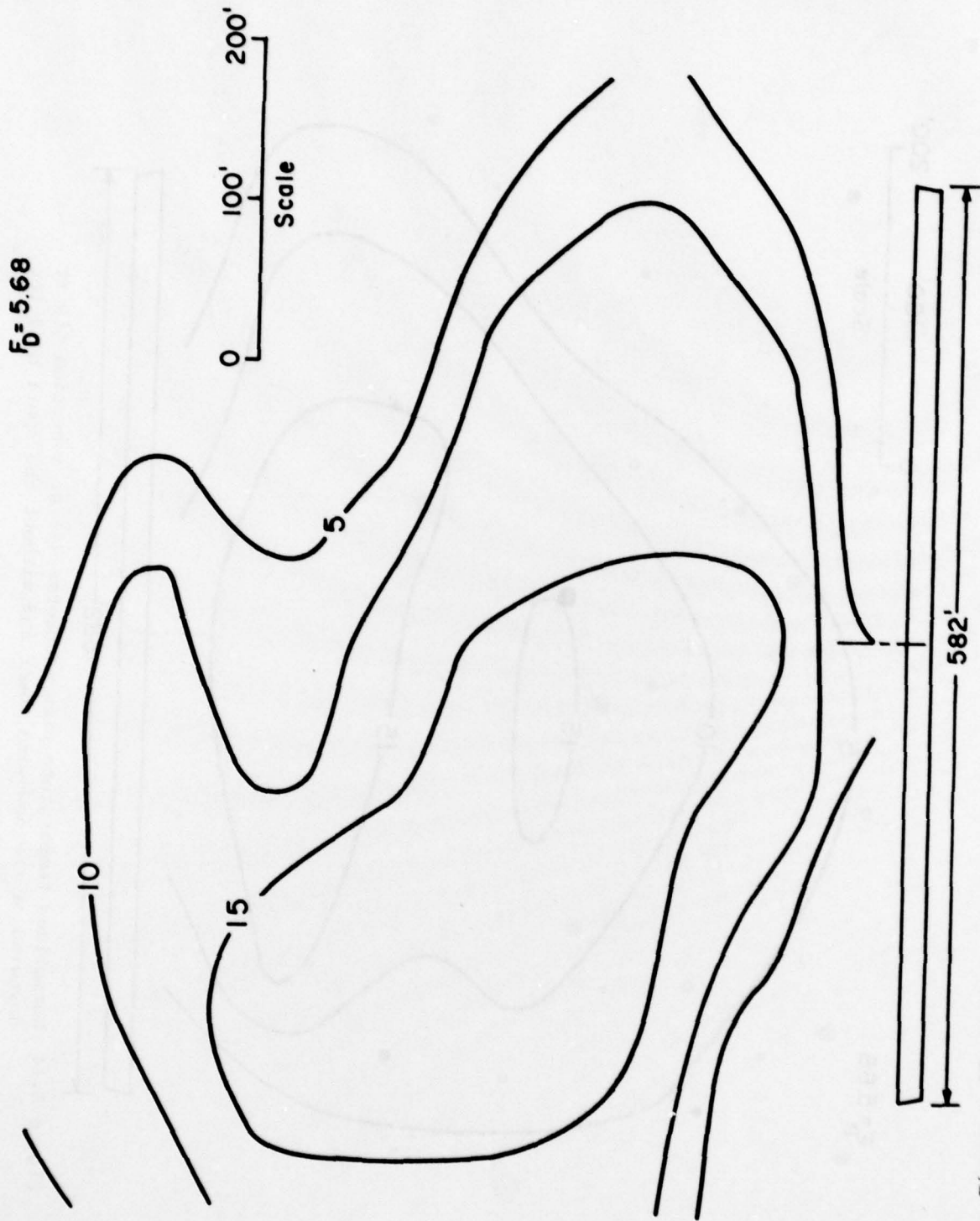
$F_D = 5.68$

Figure A.13 Normalized temperature rise isotherms (%) at a section 550 ft downwind of the downwind tower and without the spoil hill for $F_D = 5.68$, and K=1
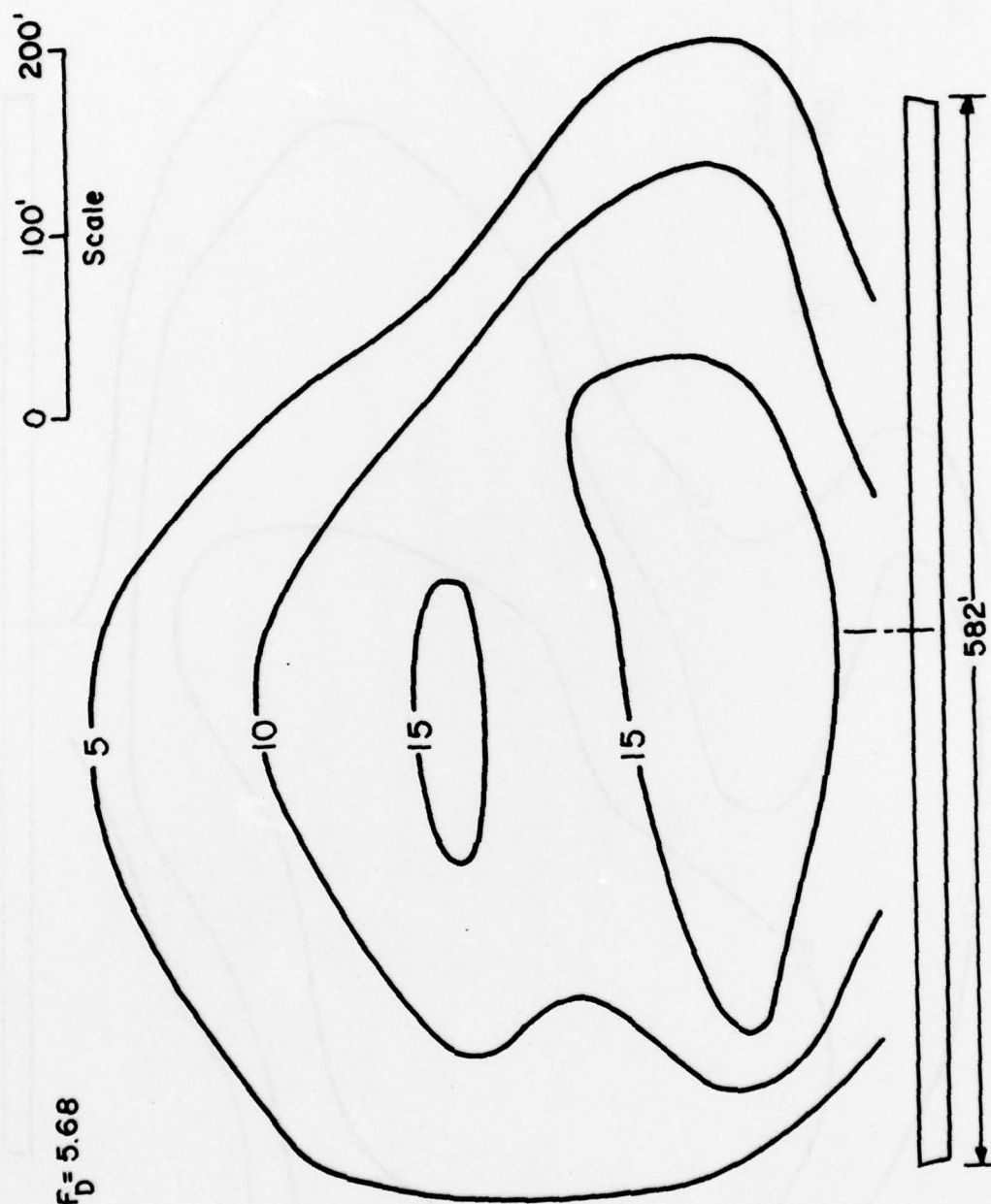
Figure A.14 Normalized temperature rise isotherms (%) at a section 550 ft downwind of the downwind tower and without the spoil hill for $F_D = 5.68$, and $K=2$
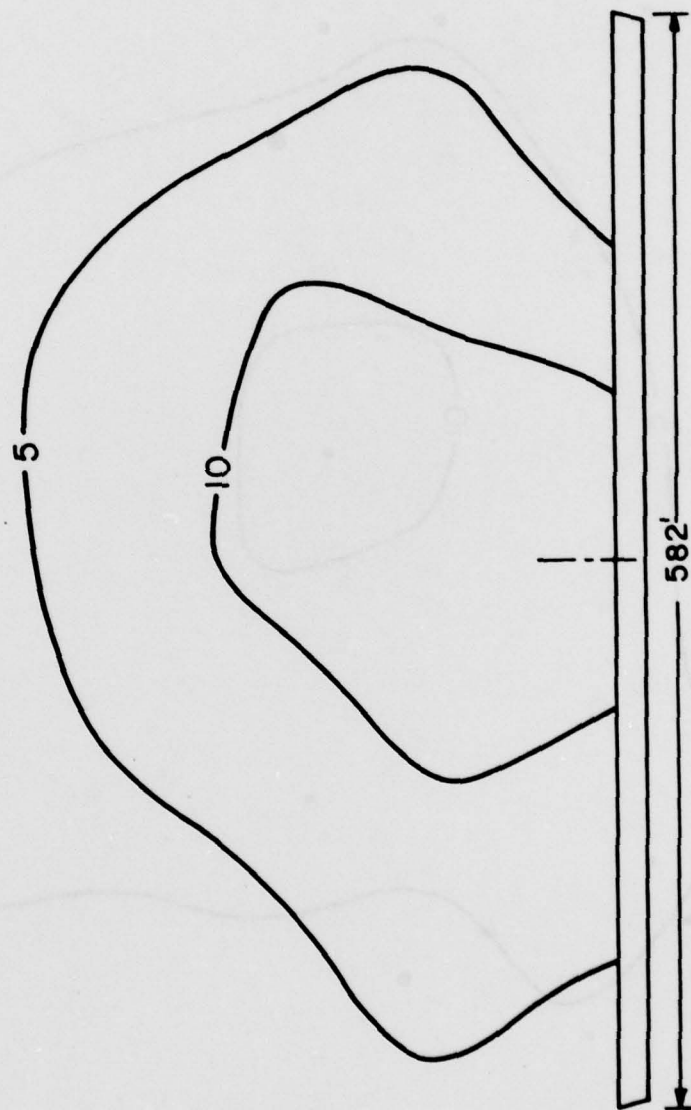
Figure A.15 Normalized temperature rise isotherms (%) at a section 550 ft downwind of the downwind tower and without the spoil hill for $F_D = 5.68$ and $K=4$
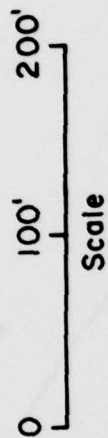
$F_D = 4.26$

Scale
0   100'   200'

5

10

582'

Figure A.16 Normalized temperature rise isotherms (%) at a section 1000 ft downwind of the downwind tower and with the spoil hill downwind of the towers for $F_D = 4.26$, and $K=1$
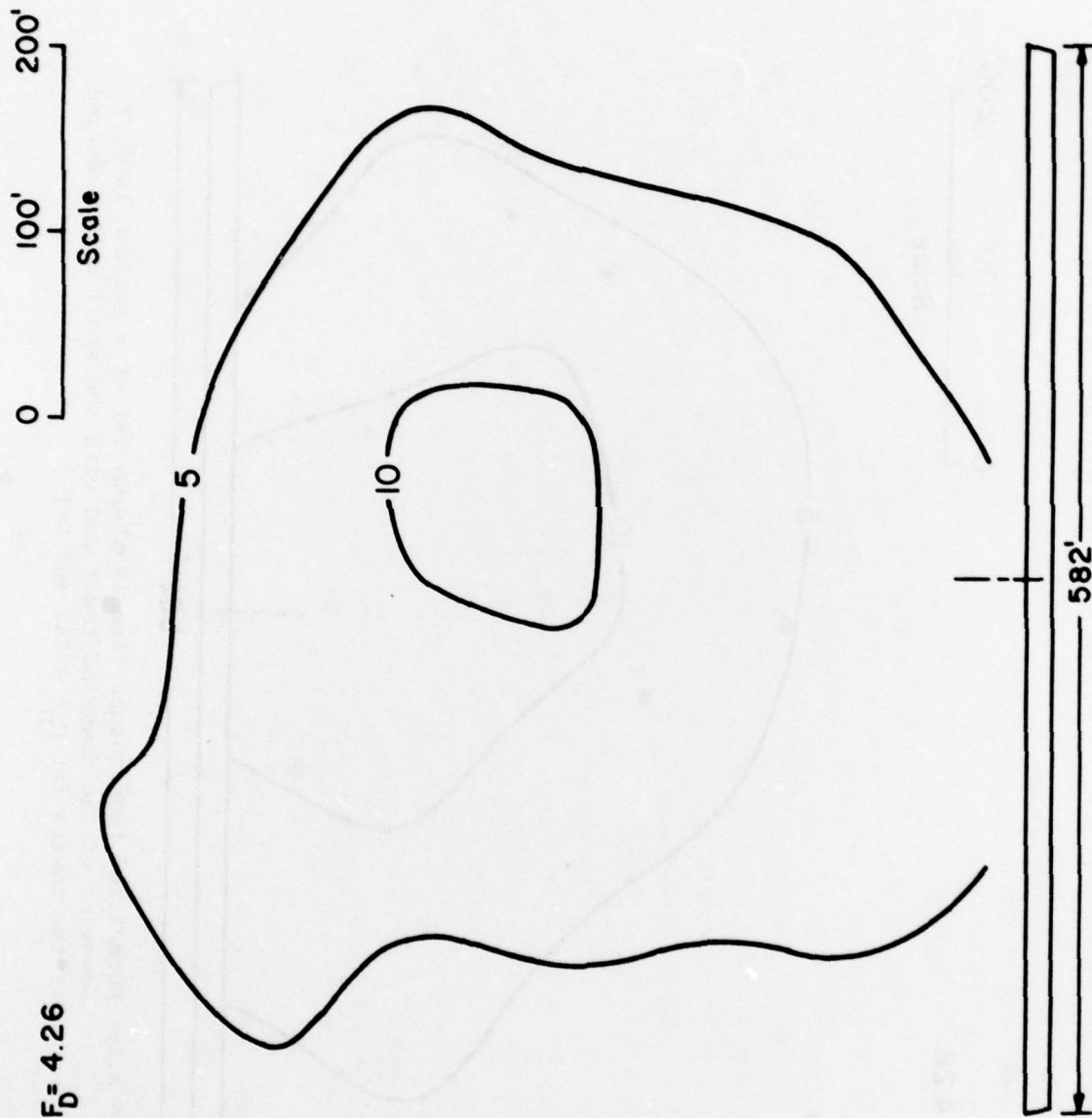
Figure A.17 Normalized temperature rise isotherms (%) at a section 1000 ft down-wind of the downwind tower and with the spoil hill downwind of the towers for F_D = 4.26 and K=2
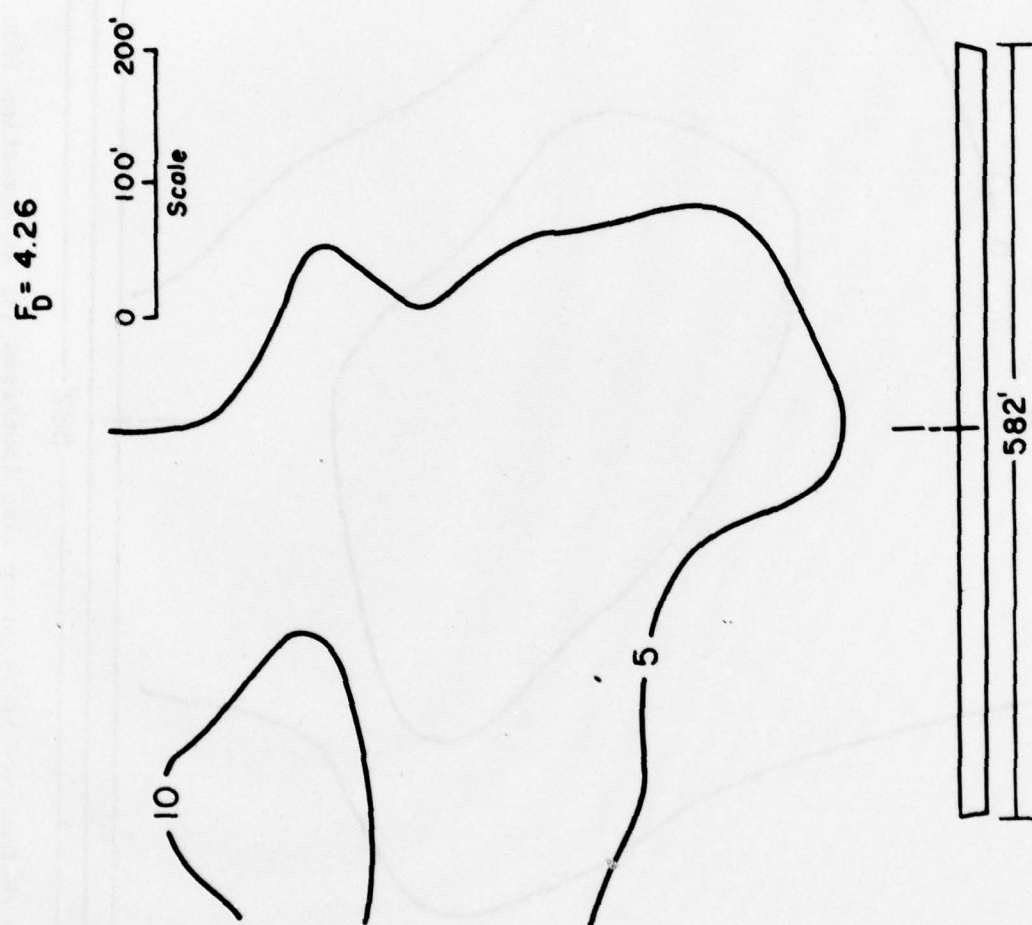
Figure A.18 Normalized temperature rise isotherms (%) at a section 1000 ft downwind of the downwind tower and with the spoil hill downwind of the towers for F_D = 4.26 and K=4
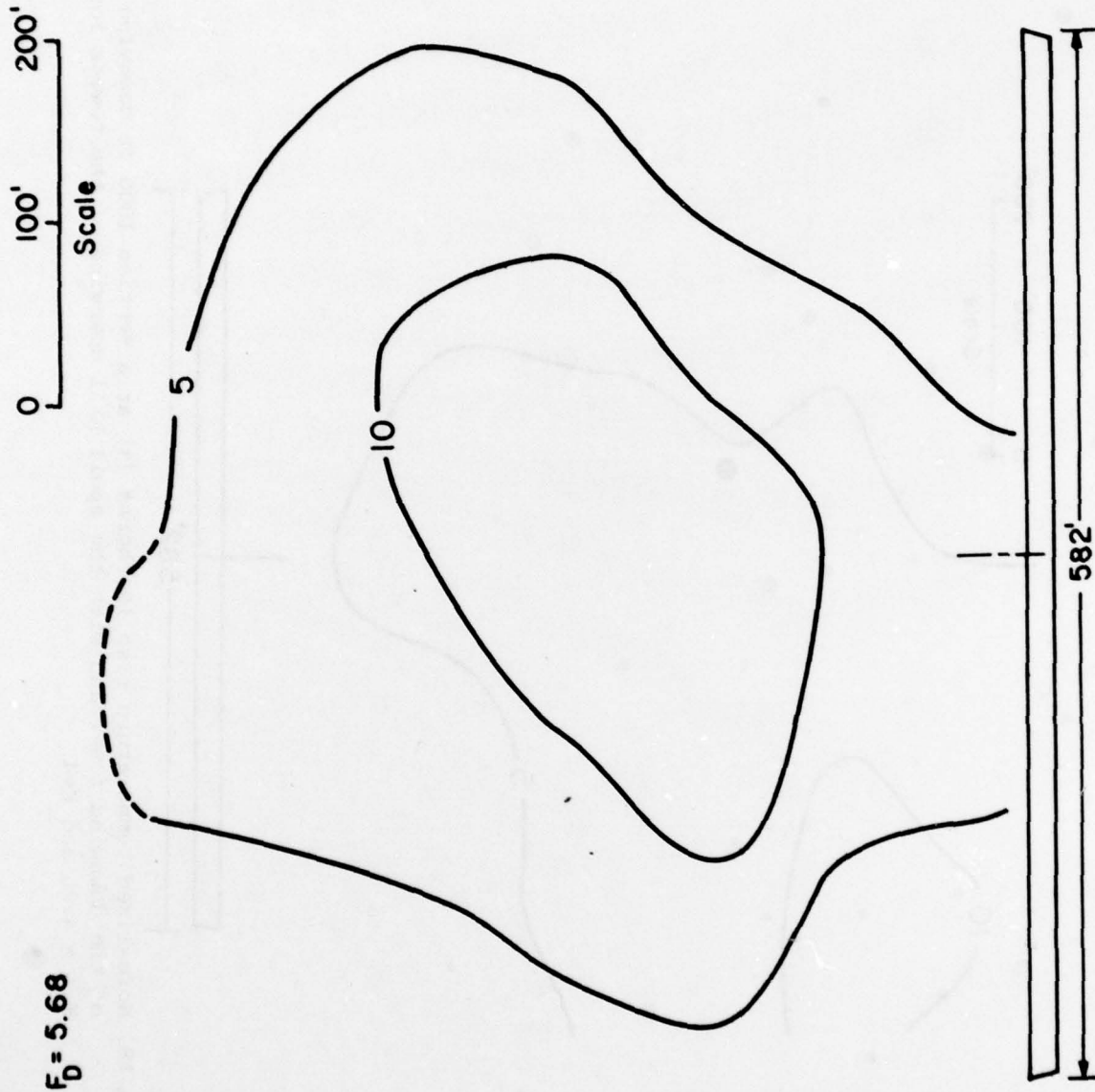
Figure A.19 Normalized temperature rise isotherms (%) at a section 1000 ft downwind of the downwind tower and with the spoil hill downwind of the towers for $F_D = 5.68$ and $K=2$